SOHO AND THE GREAT OBSERVATORY

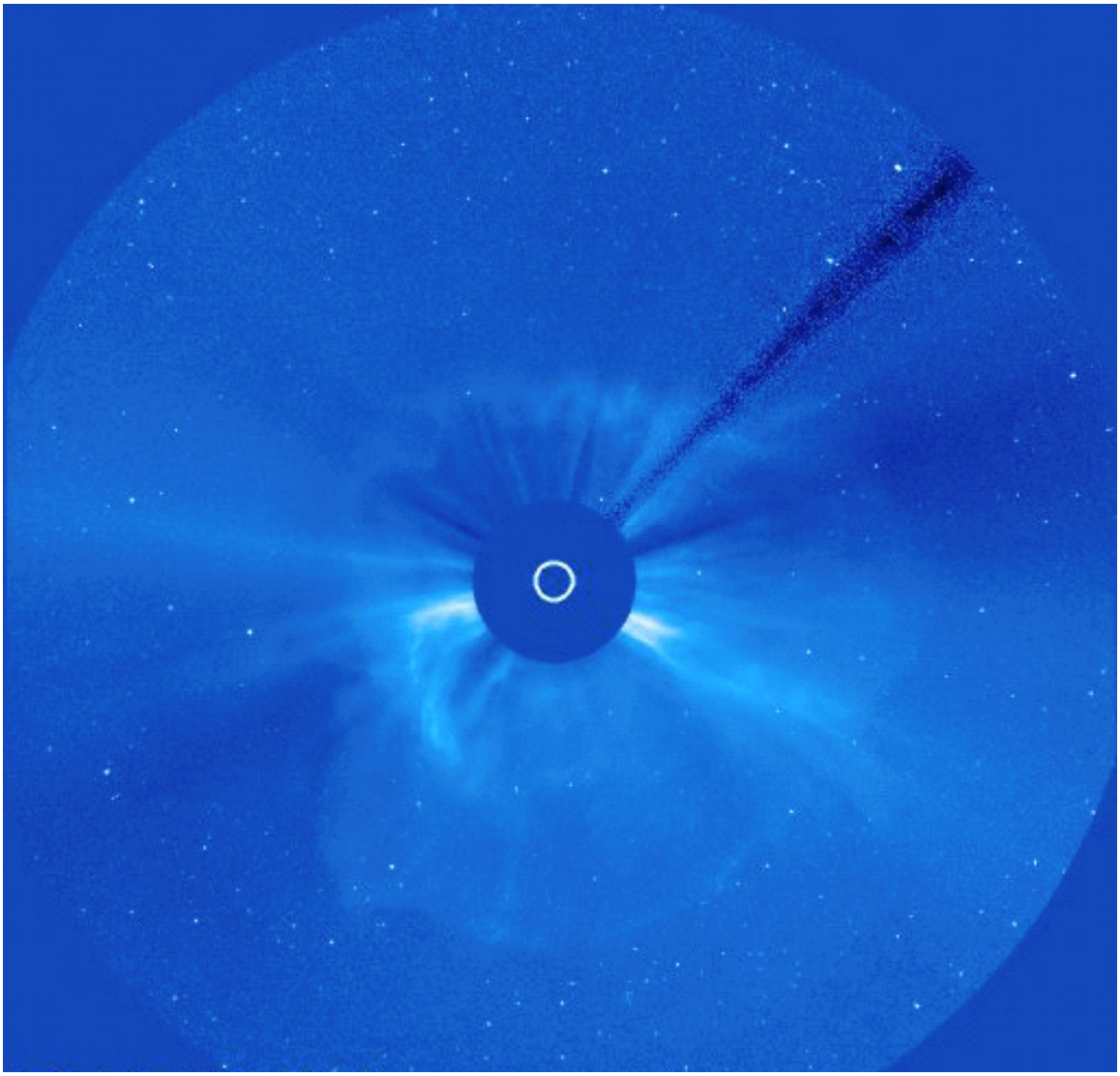

A PROPOSAL TO THE SENIOR REVIEW OF SUN-SOLAR SYSTEM CONNECTIONS OPERATING MISSIONS, 2005 OCTOBER.

Table of Contents

I. Executive Summary 1
II. Data Accessibility 2
III. Scientific Insights from *SOHO*, 2003 – 2005 2
IV. *SOHO* Scientific Objectives, 2006 – 2010 23
V. Technical and Budget, FY06 – FY10 27
VI. Education and Public Outreach 30

Appendices
A. *SOHO* publication record, 1996 – 2005Q3 34
B. Instrument Status as of 2005 September 20 35
C. Acronyms 39

Cover illustration. Halo coronal mass ejection of 2005 September 1, as observed by the *SOHO* LASCO C3 coronagraph.

Solar and Heliospheric Observatory (SOHO)

Presenters: J.B. Gurman, US Project Scientist for *SOHO*

I. Executive Summary

The current complement of Sun-Solar Systems Connections (S3C) spacecraft has been recognized as a "Great Observatory" that provides an unprecedented tool for understanding the physical conditions in our solar system, from the deep interior of the Sun to the edge of the interstellar medium. Like many of its sister ships in this brilliant constellation, *SOHO* has enabled many beautiful and startling discoveries that have helped to make us aware of just how connected disparate parts of the heliosphere really are. In the next four years, major, new solar observatories will take their place in the spaceborne Observatory, and the capabilities of *some SOHO* instruments will begin to be eclipsed – but not all, and not all at once. Even after the launch of the Solar Dynamics Observatory (SDO), *SOHO*'s lineal descendant, there will be a continuing requirement for some observations that will remain unique to *SOHO*.

In the next section of this proposal (Section II), we summarize the widespread use and easy accessibility of *SOHO* data.

We discuss in Section III a few of the many scientific insights gained from *SOHO*, often in conjunction with measurements from other spacecraft or ground-based facilities, over the last two and a half years. We believe that research using *SOHO* observations has made major strides toward understanding the solar interior, the heating of the corona, and the acceleration and composition of the solar wind — but much remains to be done.

In Section IV, we examine how closely aligned the *SOHO* scientific program is with the Research Focus Areas and Investigations proposed in NASA's current S3C Roadmap. In addition, we give just a few examples of the scientific promise of continuing the *SOHO* mission past a single solar cycle.

Section V contains the "technical/budget" information for the current baseline and enhanced options for continued scientific and mission operations during the exciting years in which STEREO and Solar-B will join *SOHO* in providing new insights into the physics of the Sun and heliosphere. After the launch of SDO, we propose to continue observations with instruments with analogs on SDO for up to a year, to facilitate intercalibration. We also provide a preview of a "Bogart" mission in which *SOHO* continues to provide LASCO coronagraph observations to supply the missing element of the SDO program in a much lower cost program. To keep *SOHO* scientifically productive through 2009, we propose to automate as much of mission operations as prudent risk management allows.

Our Education and Public Outreach proposal can be found in Section VI.

Appendices summarize the *SOHO* publication record (Appendix A) and the status of the *SOHO* instruments (Appendix B). Appendix C contains a list of acronyms.

The following individuals were among those involved in the writing of this proposal on behalf of the *SOHO* Science Working Team: J.B. Gurman and J. Brosius (GSFC), J. Kohl, S. Cranmer, J. Raymond, L. Strachan (SAO), F. Ipavich (U. Md.), P. Scherrer and A. Kosovichev (Stanford U.), and R. Howard and J. Cook (NRL). We had many helpful comments, and substantial scientific input from our European colleagues B. Fleck (ESA), R. Lallement and E. Quémerais (SdA), W. Curdt (MPS), C. Fröhlich (PMOD/WRC), A. Gabriel (IAS), A. Fludra (RAL), B. Klecker (MPE), H. Kunow (U. Kiel), and J. Torsti (U. Turku). We would also like to thank several S3C Guest Investigators who provided material for this proposal.

II. Data Accessibility

Ubiquity. *SOHO* enjoys a remarkable "market share" in the worldwide solar physics community: over 2,200 papers in refereed journals since launch (not counting refereed conference proceedings, which generally duplicate journal articles), representing the work of over 2,300 individual scientists. Even accounting for the number of "heliospheric" papers and authors in those numbers, it is not too much of an exaggeration to say that virtually every living solar physicist has had access to *SOHO* data.

Accessibility. We can assert that with confidence because all the *SOHO* experiments make all their data available, online, on the Web, through the *SOHO* archive and PI sites. A typical PI site, the EIT Web catalog, has served over 1.36 Tbyte of data since early 2003 — and the EIT database is only 540 Gbyte as of 2005 September. The Solar Data Analysis Center (SDAC) has also shipped the *entire* EIT dataset (another 1.5 Tbyte) to three users who wished to examine substantial fractions of the dataset and had sufficient local storage capacity to copy the data and return the media. The larger MDI database, which includes several levels of computationally expensive, higher-level data products, contains some 20 Tbyte of data products, and has served over 9 Tbyte in response to nearly10,000 online data requests in the last two years. (This total does not include larger data exports shipped to Co-Investigator and Guest Investigator sites on tape.) In addition to professional access, amateurs routinely download LASCO FITS files and GIF images to search for new comets. As a result, nearly half of all comets for which orbital elements have been determined (since 1761) were discovered by *SOHO*, over two thirds of those by amateurs accessing LASCO data via the Web. An Italian amateur, T. Scarmati, discovered the 1,000th *SOHO* comet on 2005 August 5. To help publicize comet science, the *SOHO* project held a contest in the months before the discovery that allowed the public to guess the date and time of perihelion passage for *SOHO*-1000.

Research access. All *SOHO* instruments' scientific data are accessible through a single interface, http://soho.nascom.nasa.gov/catalog/ . This searches both the general *SOHO* archive at the Solar Data Analysis Center (SDAC) at Goddard, and the MDI high-rate helioseismology archive at Stanford. (MDI full-disk magnetograms obtained every 96 minutes are part of the general archive, because of their usefulness for solar activity-related research.) In both archives, the holdings are identical to those used by the PI teams, and are current (*i.e.* to within a month or two before present, to allow time for "Level-Zero" data delivery.) *SOHO* data at both the SDAC and the Stanford Helioseismology Archive were among the first data whose metadata, including browse images for EIT and MDI, became searchable *via* the Virtual Solar Observatory (VSO). The VSO is designed to deliver data *via* the original servers, so the download traffic still occurs at those sites.

Publications. The *SOHO* publications database can be accessed at:
http://sohodata.nascom.nasa.gov/cgi-bin/bib_ui .

III. Scientific Insights from *SOHO*, 2003 - 2005

The following, brief descriptions of scientific insights gained from *SOHO* have been gleaned from papers published in, or recently submitted to, refereed journals since the 2003 Senior Review; a few results from recent conference proceedings are also included. Scientific insights from earlier phases of the mission were covered in the proposals to the 1997, 2001, and 2003 Senior Reviews.

The Solar Interior and Total Irradiance

Total Solar Irradiance

The nearly 10 year long total solar irradiance (TSI) record from the VIRGO radiometers, and important differences in their designs allowed the PI team to develop a model (Fröhlich 2006) for the degradation and other exposure dependent changes, which implicitly takes the dose of radiation received by the detectors into account. The model is able to account for both long-term degradation of response and for an initial increase in measured TSI due to an increase of the absorptance of the precision aperture and hence an increase of the temperature and the corresponding IR radiation emitted into the cavity for *any* radiometer of similar design to VIRGO PM06V (*e.g. SMM* ACRIM-I and NIMBUS-7). So it is now possible to correct the results of these radiometers accordingly, and hence construct a more reliable composite TSI record over the last 26 years, as shown in Figure 1. The final result could never have been achieved without the very reliable TSI record of VIRGO, not only by the contribution of its record since 1996, but also by the model developed for the different exposure dependent changes of present space radiometers.

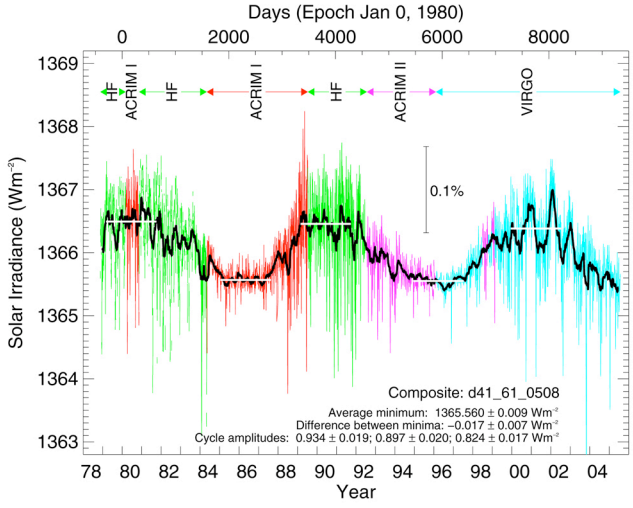

Figure 1. The composite total solar irradiance (TSI) for over two solar cycles, combining data from multiple spacecraft instruments, and made possible via the application of a new model of instrument performance. Different colors indicate different data sources.

From this composite record, it now appears that *(i)* there is no evidence for a long-term, secular trend, since the difference between the last two minima is not significantly different from zero at the 5-sigma level, and *(ii)* the average amplitudes of the three cycles are within 10% and slightly decreasing from 0.93 to 0.82 Wm^{-2}, although each maximum looks quite different.

The Solar Interior

Constraints on solar abundances. Recent determinations (Asplund *et al.* 2004, Asplund *et al.* 2005a, Lodders 2003) of the abundances of heavy elements have led to significant changes in our understanding of the internal structure and constitution of the Sun. Standard solar models calculated with the new abundances are significantly different from the helioseismic results which were in a good agreement with the previous solar models. Figure 2 shows the relative difference between the *SOHO* MDI measurements of the sound speed profile inside the Sun and various solar models. The solid curve shows the

difference for a standard solar model with the previously known solar composition. The dotted curve shows this difference for the standard model computed with the new composition which has lower abundances of oxygen and iron as determined by Asplund *et al.* (2005a,b).

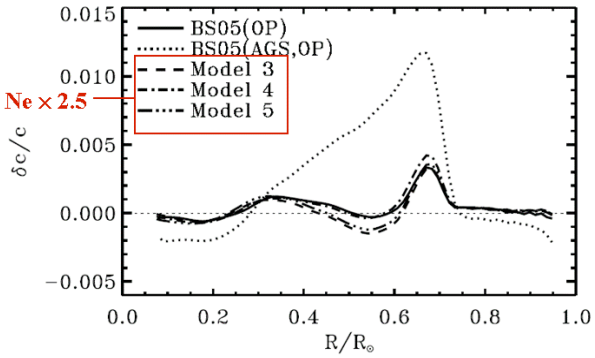

Figure 2. Relative sound-speed differences, between some selected solar models and helioseismological results from MDI data. The BS05(OP) (solid curve) is a standard solar model calculated with the previously known abundances of helium (0.2725) and heavier elements (0.0188). Model BS05(AGS,OP) (dotted curve) is a solar model calculated with the newer and lower heavy-element abundances (Y=0.2599, Z=0.0140). Models 3, 4, and 5 are calculated with the increased relative abundance of neon show an agreement with helioseismology data which is comparable to that of the previous standard solar model, BS05(OP) (from Asplund et al. *2005a).*

This discrepancy represents a new challenge for helioseismology and solar modeling, and also affects the predicted neutrino fluxes (Bahcall and Serenelli 2005, Bahcall *et al.* 2005, Guzik *et al.* 2005, Turck-Chièze *et al.* 2004a). One possible solution is to increase the relative abundance of neon by a factor of 2.5 (Antia and Basu 2005). This may compensate for the lack of oxygen and iron as shown in Fig.1 by Models 3-5 calculated by Bahcall *et al.* (2005).

Obviously, more precise helioseismic measurements of the solar structure are required to provide more accurate constraints for the solar composition. This can only be achieved by using longer time series of observations of solar oscillations to determine the frequencies of global acoustic (*p*) modes, and correcting their solar-cycle variations, more accurately.

Rotation of the deep interior. Inversion analysis of the rotational splittings of *p*-modes enables the determination of the core rotation as a function of depth. Analyzing *SOHO* GOLF data in this way, Couvidat *at al.* (2003) obtain results that are consistent with a flat (solid-body) rotation rate of the inner layers down to around 0.2 R_{Sun}.

The continuing search for g-modes. The search for solar g-modes (in which buoyancy is the restoring force), which if found would vastly improve uncertainties for the solar core, continues as the length of the data-base increases. No *g*-modes have yet been positively identified, although some candidates have been found in the GOLF observations. The upper limit for these modes may be as low as 2 mm s^{-1}, based on the search for multiplets (Turck-Chièze *et al.* 2004b). These figures are more than an order of magnitude lower than pre-*SOHO* claims.

Solar-cycle variations in the size of the Sun: an unexpected limit to total irradiance variations. Helioseismic observations from space provide a unique opportunity for measuring oscillation frequencies of surface gravity waves (the *f*-mode) of medium angular degree *l*, which represent a very sensitive indicator of variations of the stratification just below the surface of the Sun. These data are very important for diagnostics of subsurface, solar-cycle effects and mechanisms underlying total irradiance variations. The medium-*l f*-modes are not observed from the ground because of their relatively low amplitude. Figure 3 shows the estimates of the variations of the radius of the subsurface layers of the Sun with the activity cycle, obtained by Lefevbre and Kosovichev (2005), following the theory of Dziembowski and Goode (2004). It appears that the changes in the solar stratification due

to solar activity are not uniform with depth. There is evidence for a compression layer at the depth of 7 Mm (0.99 R_{Sun}). It is intriguing that the most significant changes occur below the solar surface. According to these inferences, the Sun is smaller at activity maximum, and the variations of the surface radius do not exceed 2 km.

By analyzing changes of the oscillation frequencies of the solar acoustic (*p*) modes, obtained from *SOHO*/MDI data, Dziembowski and Goode (2005) concluded that the Sun not only becomes smaller at solar maximum but also cooler in the subsurface layers. VIRGO TSI measurements during the same period, however, show a total solar irradiance increasing

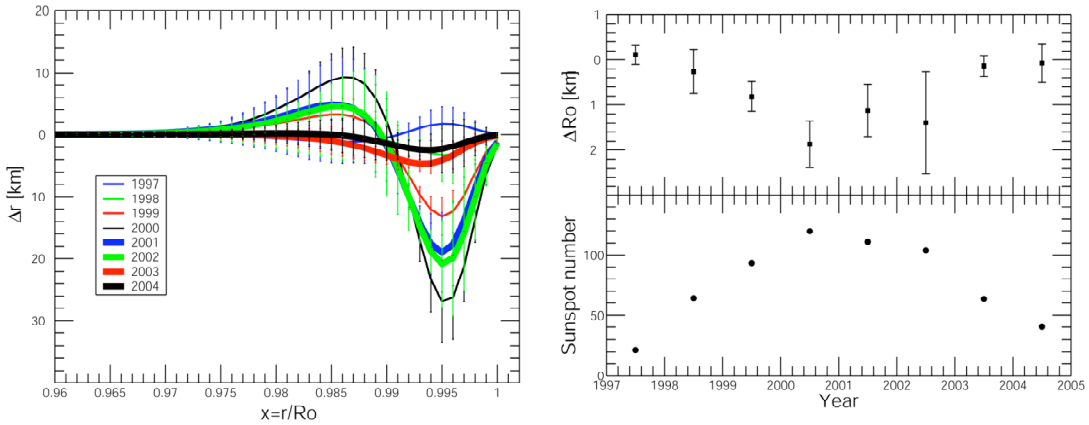

Figure 3. The left *panel shows changes of the radius of subphotospheric layers with the solar cycle (relative to the solar minimum values of 1996) for the whole period of SOHO/MDI observations, inferred by helioseismic inversion of frequencies of f-modes (surface gravity waves). The* right *panel shows the solar radius estimated at the surface changes in antiphase with the sunspot number, meaning that the Sun becomes smaller at the activity maximum.*

with increasing solar activity. The solution to the apparent paradox of a smaller and cooler Sun radiating more lies in surface corrugation as a product of the nonuniform distribution of magnetic field – that is, the surface area increases even as the radius shrinks slightly. The deviations from spherical structure can be also estimated from the helioseismology data, in particular, from frequency splitting, and from the full-disk continuum intensity images. By putting together these constraints Dziembowski and Goode were able to put an upper limit on the possible increase of total solar irradiance (TSI) due to solar activity. This limit is

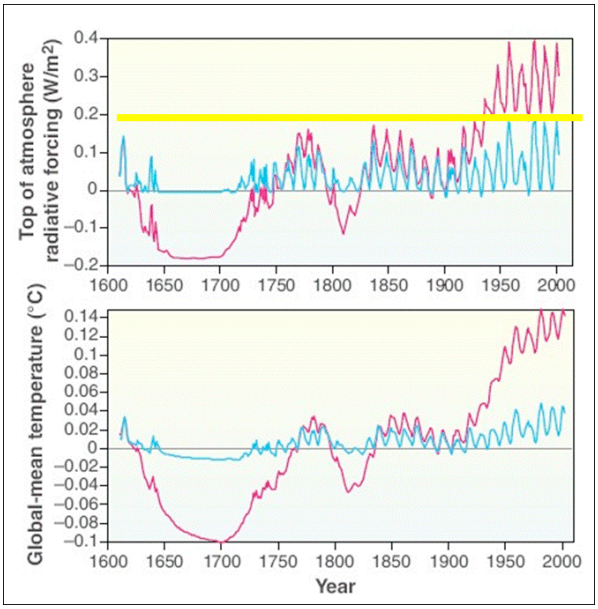

Figure 4. The upper blue curve shows the irradiance variation assuming variations in the past track those over the last two cycles and the red curve includes the putative long term component. This is translated to temperature changes using the NCAR model (Foukal, et al. 2004). With the long term trend, one can account for part of the cooling over the first half of the 20th century and the depths of the Maunder minimum. Foukal et al. (2004) deny the presence of the longer-term component on phenomenological grounds: the magnetic network discovered by Hale in the 1890's would have had to disappear during the 1920's).

shown by the yellow line in Figure 4, which also shows the irradiance variations during the past four hundred years, assuming that variations in the past track those over the past two cycles (blue curve), and the changes that could explain the climate variations and might be caused by some unknown, long-term processes on the Sun, as suggested by Foukal *et al.* (2004).

This limit, derived from helioseismology, significantly constrains possible irradiance changes. If our current understanding of cycle-driven solar structure and size variations accounts for all the physics of TSI change, we can put a hard upper limit on the changes in TSI (yellow line). Increases in irradiance are bound directly by increases in activity. Since higher activity cycles are shorter and there is Greenland ice core data showing a roughly 11-year cycle going back over 100,000- years, it is unlikely that the Sun's irradiance over historical times was much greater than it is now. Thus, we must explain how there can be terrestrial signatures of the solar cycle when the irradiance changes are too small to "force" them. We therefore need to carry out joint helioseismology and irradiance observations on *SOHO* for the declining phase of the current solar cycle and during the transition to the new cycle – problems in merging groundbased helioseismology network data prohibit this sort of analysis on those data, and TSI can only be measured accurately from space.

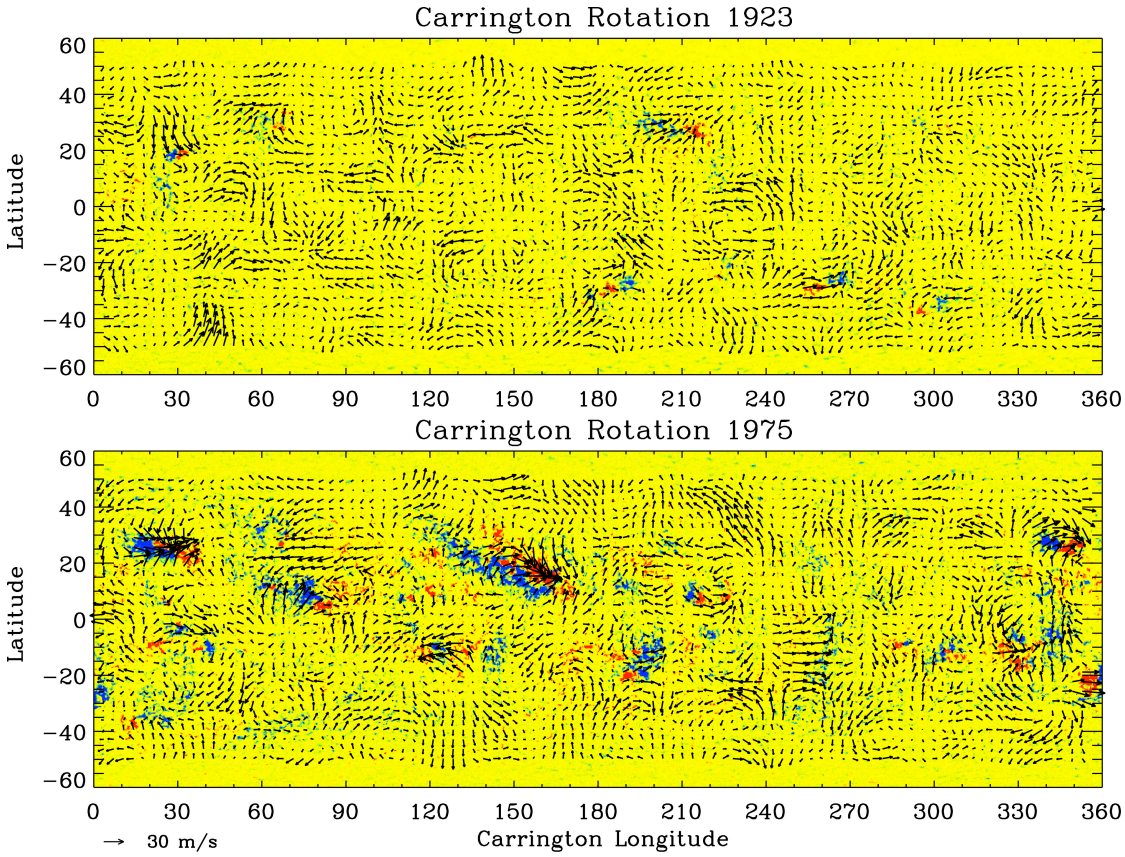

Figure 5. Synoptic maps of large-scale subphotospheric flows obtained from SOHO/MDI during the activity minimum (upper *panel) and activity maximum* (lower *panel). The colored background shows the corresponding synoptic maps of the photospheric magnetic field: positive (red) and negative (blue) polarities. Magnetic activity near the solar surface appears to be associated with substantial changes in the subsurface flow patterns ("subsurface solar weather").*

Subsurface solar weather changes with the solar cycle. New methods of local helioseismology (time-distance helioseismology, helioseismic holography, and ring-diagram analysis) provide a unique, three-dimensional view of the solar interior. The 3-D imaging of the solar interior requires an uninterrupted series of stable Dopplergrams. Attempts to apply these methods (particularly, time-distance helioseismology and helioseismic holography) to data from the groundbased networks have not been as successful as analysis of the MDI data, which have revealed a fascinating picture of the large-scale, subsurface dynamics of the Sun. Now, dramatic changes with the solar cycle (Haber 2003, 2004; Hindman *et al.* 2004a,b; Zhao and Kosovichev 2004a, b) have been detected. Figure 5 gives an example of the differences in the subsurface flow pattern for two solar rotations during the solar minimum (upper panel) and solar maximum (lower panel).

The synoptic flow maps are obtained from the MDI Dynamics Program run during continuous contacts with *SOHO*, and represent a valuable source of information about the mechanisms of solar activity in the interior (Haber 2004, Zhao and Kosovichev 2004a). These maps are provided to the solar physics community and are being studied along with the traditional synoptic maps of solar magnetic fields and new coronal EUV maps constructed from *SOHO* EIT data (Benevolenskaya 2003). The synoptic studies of the Sun are particularly important for understanding the basic mechanisms of the solar dynamo and links to the coronal and heliospheric activity. We expect more detailed maps of subsurface flows to be produced from SDO HMI measurements, but until those are available (late 2008 or early 2009 at the earliest), we need to extend *SOHO* MDI local-area helioseismology and longitudinal magnetic field measurements to provide continuity of this new source of information on solar magnetic variability.

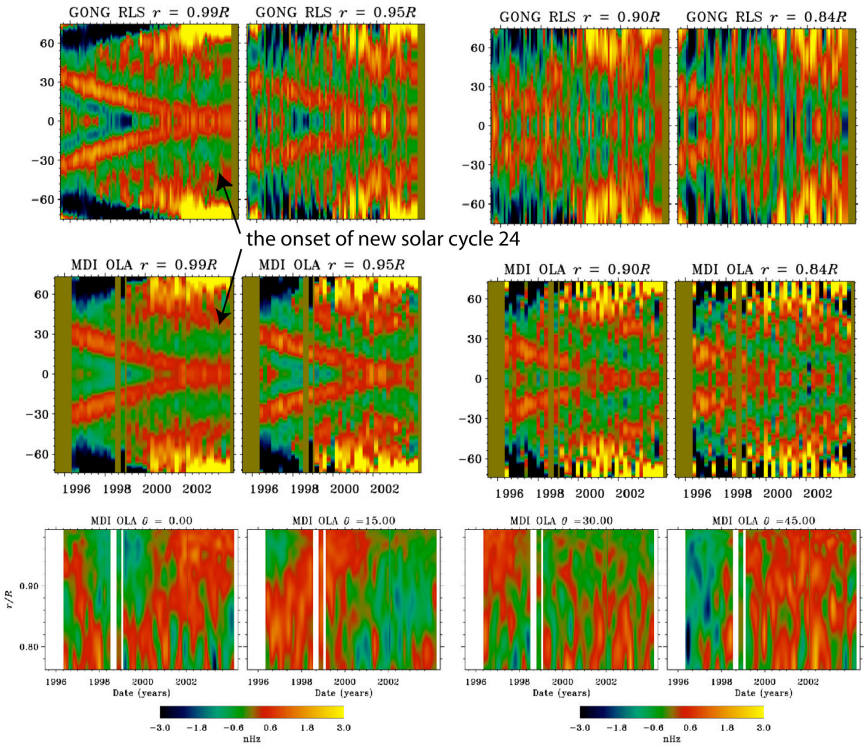

Figure 6. Time-latitude (top and middle panels) and time-radius maps of the zonal flows ("torsional oscillations") obtained by helioseismic inversions from GONG and MDI data.

Global circulation, solar dynamo, and prediction of the solar cycle. Internal differential rotation and meridional circulation are the most important components of the solar

dynamo. Dynamo models of the solar cycle predict that the toroidal magnetic field of the Sun, which is the source of active regions and sunspots, is generated by the differential rotation and that the polarity of the dipole poloidal field is reversed every eleven years due to the magnetic flux transport to the polar regions by the meridional flow. Helioseismic observations for *SOHO* MDI and also from the ground-based GONG network have detected changes in the zonal flow pattern in the convection zone of the Sun (Howe *et al.* 2004), shown in Figure 6.

The zonal flows play an important role for solar activity because active regions tend to appear in the transition shear layers between faster (red) and slower (green) streams. MDI observations (middle and bottom panels) provide better resolution in deeper layers (at and below $0.95R_{Sun}$). It is, however, essential to continue this type of helioseismology measurement from both MDI and GONG because these independent observations provide confidence in the detection of weak but significant features, such as the appearance of new branches of torsional oscillations at high latitude in 2002, indicating the onset of the next solar cycle well before the appearance of new cycle sunspot regions. The MDI observations indicate that these new branches originate in the deep convection zone. The origin of the evolving zonal flows is not yet understood.

A late appearance for the next cycle? Haber *et al.* (2002) and Zhao and Kosovichev (2004b) discovered that the meridional flow slows down as the solar cycle progresses. After the solar maximum in 2001 the flow speed becomes higher again. This discovery is important for flux-transport dynamo theories which assume that the magnetic polarity reversal in the Sun's polar regions are caused by the transport of magnetic flux by the meridional flow. The deceleration of the meridional flow therefore results in a delay of the next solar cycle. According to the dynamo theory calculations (Dikpati *et al.* 2004) the next solar cycle will start in late 2007 or early 2008 (Figure 7), six to twelve months later then the current NOAA Space Environment Center prediction.

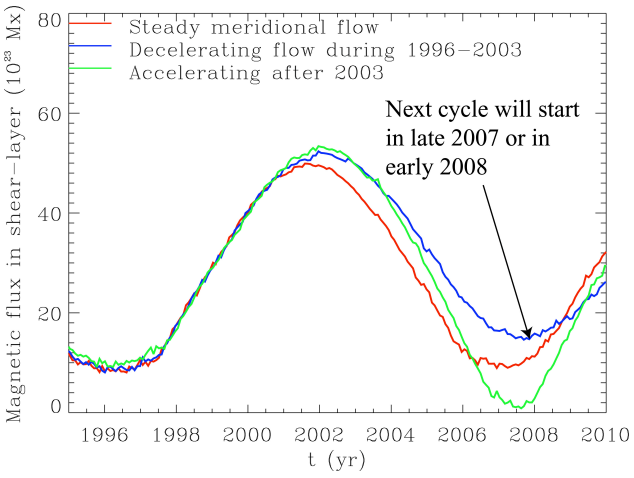

Figure 7. Magnetic field flux calculated using a dynamo model for various models of the meridional flow. The results for the meridional flow determined from the MDI helioseismology data (blue) predict that the next cycle will start in late 2007 or early 2008.

Evolution of active regions. Local-domain helioseismic studies have revealed global-scale flows beneath the solar surface. These flows of Solar Subsurface Weather (SSW) are complex and exhibit rich time dependence. Maps of SSW made with ring analysis reveal large-scale patterns of converging and diverging flows, as well as large jets and circulation patterns. Previous studies have observed these phenomena in the vicinity of active regions, but questions remain regarding correlations between flow patterns and active region characteristics. Most active regions show converging flows near the surface but exhibit greater variation at depth. Some of the active regions are marked by inflows at all depths,

some possess surface inflows and deeper outflows, and some show strong jets. Such flow variations among different active regions are quite striking (Brown et al. 2004).

The MDI team has begun a systematic statistical study of SSW flows around active regions observed during MDI dynamics observing programs. The primary goal is the understanding of the life cycle of active regions and relationship between the internal dynamics of active regions and their magnetic structure and flaring and CME activity at various phases of the solar cycle. Patterns of flow behavior that may precede rapid magnetic reconfiguration are of particular interest to us. Large-scale flows could, for example, lead to a gradual evolution of magnetic topology until a highly unstable configuration is achieved, which then rapidly reconnects.

Subphotospheric dynamics of flaring active regions. It is not known at present whether large-scale flows of subsurface space weather contribute to the possibility of flaring and CMEs or whether the real culprits are far smaller scales. Various techniques of local helioseismology are being used to search for subphotospheric processes related to the flaring activity. Of particular interest are measurements of the kinetic vorticity and helicity which may be related to generation of electric currents and magnetic helicity, and also detection of subsurface shearing flows which can cause shear of magnetic field and trigger instabilities. The initial results indeed show evidence for both the helicity variations and shearing flows. While the large-scale helicity variations of active regions can be measured from both MDI and GONG data, the smaller-scale shear flows have been detected only from the MDI data by the time-distance technique.

In the example, shown in Figure 8, Komm *et al.* (2004) used daily and synoptic flow maps from MDI data covering the disk passage of AR 10486 in 2003 October-November. In the synoptic maps, a strong signal in each of the vorticity components and hence in the kinetic helicity is found at the location of the active region during the epoch when the flares occur. This signal is absent from the same location in the synoptic maps before and after the flares occur. In the daily flow maps, a systematic variation in the kinetic helicity was observed at the location of AR 10486 with large values before the flare event and small ones after the event that remain rather constant. These systematic variations in synoptic and daily maps might be subsurface signatures of the flare events.

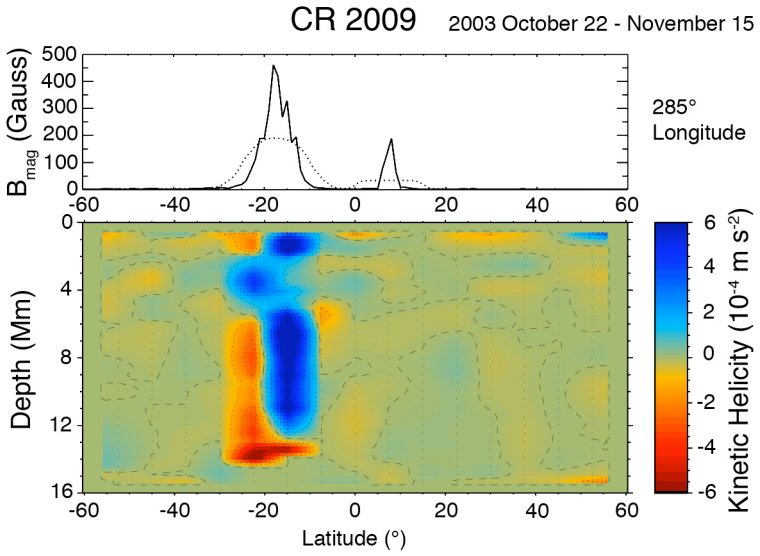

Figure 8. The kinetic helicity at 285° longitude in CR 2009 as a function of latitude and depth. Top: gross magnetic flux (solid curve) and averaged over 15° (dashed curve); bottom: kinetic helicity. The large values coincide with the location of the active region and they are significantly different from zero. The sign of the kinetic helicity remains the same at depths greater than about 5 Mm at the locations of AR 10486. Closer to the surface the sign changes with depth indicating a more complicated behavior.

Subsurface shearing flows at 4 – 5 Mm beneath active regions have been detected by time-distance helioseismology analysis of the MDI data (Dzivkacova *et al.* 2003, Kulinova *et al.* 2003), with a typical flow velocity of about 1 km s^{-1}. The precise effect of these flows on the structure and stability of magnetic fields of active regions, and their role in triggering flares and CMEs is not known. More observations, data analysis and numerical modeling are necessary to establish this. However, the initial results, illustrated in Figure 9 for two solar flares, reveal shearing and convergence beneath the location of magnetic energy release in the flare, as expected near polarity inversion lines of the photospheric line-of-sight magnetic field.

It appears that shearing flows tend to appear in the polarity inversion line regions where the magnetic field changes permanently during the impulsive phase of the solar flares, and only at these depths. These observations indicate that the critical coupling between the subphotospheric plasma flows and magnetic fields may occur at a depth of 4-5 Mm, and, thus, this region requires further detailed investigation, both from *SOHO* MDI and by MHD simulations such as those carried out by the CISM project.

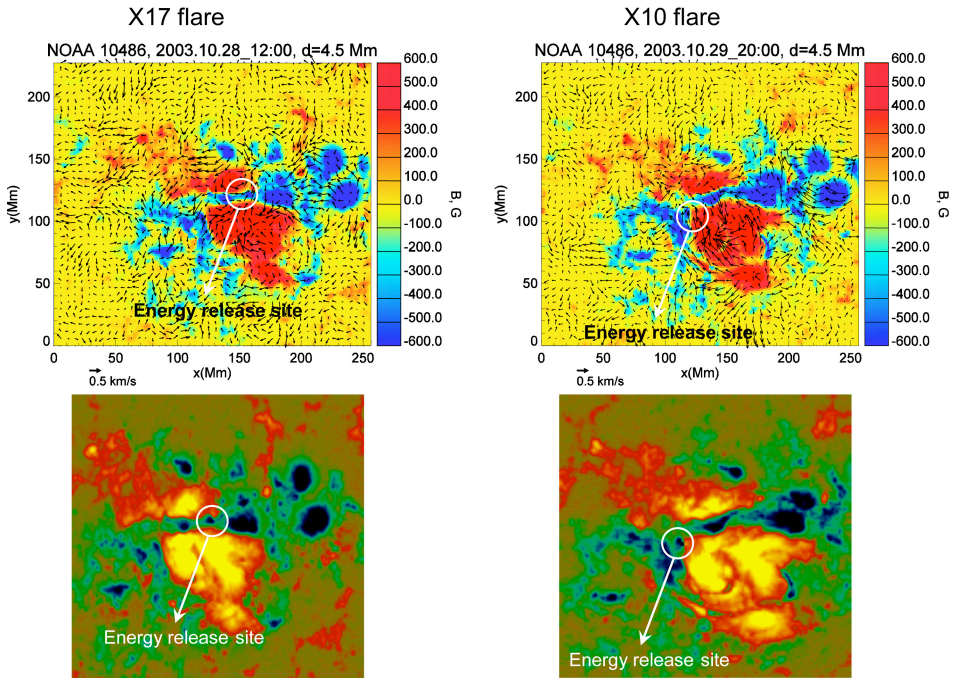

Figure 9. High-resolution maps of subsurface plasma flows obtained by time-distance helioseismology (top panels) and MDI magnetograms (background top and bottom images) during two solar flares: left, X17 (Oct. 28, 2003, 11:10 UT) and X10 flare (Oct. 29, 2003, 20:37 UT) During the flare strong plasma flows are observed at depth 4-6 Mm, shearing and converging in the magnetic neutral line region where the magnetic energy was released.

Helioseismic response to solar flares. The helioseismic response to solar flares ("sunquakes") is of significant interest because this phenomenon can provide new information about energy release and transport in flares, and also because of their potential for helioseismic diagnostics of sunspots and active regions. The first sunquake observed to result in circularly expanding waves on the solar surface was observed for a flare of 1996 July 9, the last X-class flare of the previous solar activity cycle and the first flare observed by *SOHO* (Kosovichev and Zharkova 1998). No sunquakes, however, appeared in *SOHO* observations from the start of the current cycle in 1996 until 2002, when a flare later

analyzed by Donea and Lindsay (2005) showed "egression power" or changes in the oscillation power spectrum.

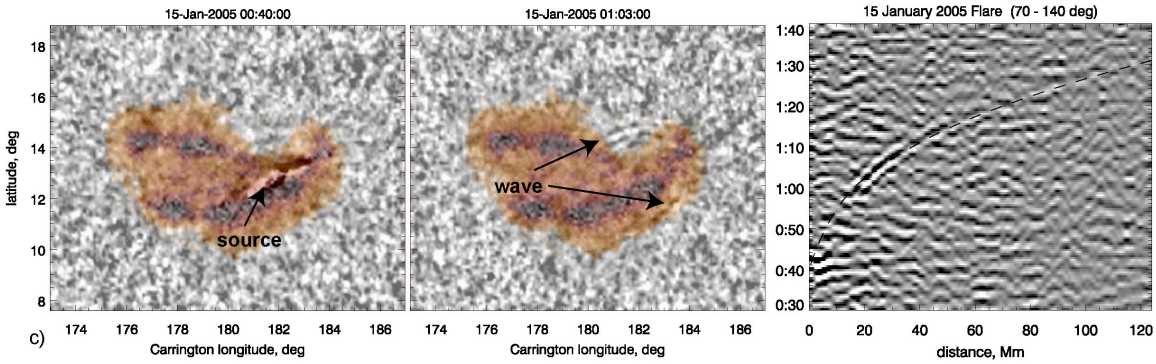

Figure 10. Observations of the helioseismic response of the Sun ("sunquakes") to the X1 flare of 2005 January 15. The left panel shows a superposition of MDI white-light images of the active region and the location of the sources of the seismic waves determined from MDI Dopplergrams, the middle panel shows the seismic waves, and the right panel shows the time-distance diagrams for this event. The dashed curve is a theoretical time-distance relation for helioseismic waves.

The X17 flare of 2003 October 28 (see Figure 9) was the first flare of the current solar cycle to produce seismic waves observable by *SOHO* MDI; similar results were obtained for two somewhat smaller flares. The three panels of Figure 10 show the observational results for one of the latter, an X1 flare of 2005 January 15. The leftmost panel shows a superposition of the MDI white-light image of the active region and the difference between two MDI Dopplergrams taken during the impulsive phase of the flare showing the location of the initial flare impacts in the photosphere. The middle panel shows the Dopplergram difference 23 minutes later, which reveals two semi-circular fronts of expanding seismic waves. The rightmost panel shows the time-distance diagram for the wave propagating northward. The comparison of the sunquake images with RHESSI observations reveals a close association between the seismic waves and the hard X-ray source, indicating that high-energy electrons accelerated during the flare impulsive phase produced strong, compressive waves (shocks) in the photosphere, in turn causing the sunquake (Kosovichev 2005). Figure 11 illustrates this sequence of events for the 2005 January 15 flare, from top to bottom. The high-energy electrons accelerated in the flare (presumably, high in the corona) produced a hard X-ray impulse in the lower atmosphere and generated downward propagating shocks which hit the photosphere and generated the seismic waves.

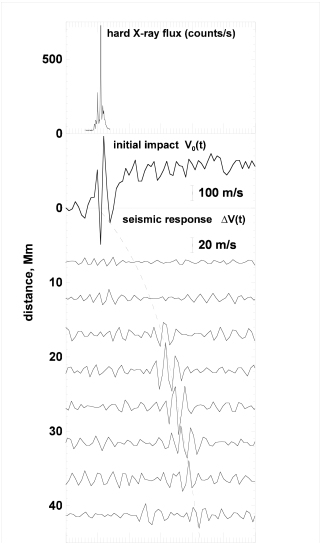

Figure 11. The sequence of events during the flare of 2005 January 15. High-energy electrons are accelerated in the solar flare and interact with the lower atmosphere, producing hard X-ray bremsstrahlung emission (observed by RHESSI) and shocks – initial hydrodynamic impact in the photosphere (observed by SOHO/MDI). Then, about 20 min after the initial impact an expanding seismic wave was detected by SOHO/MDI. The dashed curve shows a theoretical relation for helioseismic waves.

These new observations from *SOHO* and RHESSI provide unique information about the interaction of the high-energy particles associated with solar flares with the dynamics of the solar atmosphere during and after the impulsive phase of the flares. These data also provide unique information about the interaction of acoustic (MHD) waves with sunspots, showing explicitly propagation of wave fronts through sunspot regions. These observations provide the prospect of new methods of helioseismologic analysis of flaring active regions, similar to the methods of seismology used to study earthquakes.

The Solar Atmosphere

Surprisingly strong magnetic field above a sunspot. Brosius and White (2005) have obtained coronal magnetic field strengths of 1750 G at a height of 6 Mm and 960 G at 12 Mm above a pair of large sunspots, by combining microwave observations of third harmonic gyroemission at 15 GHz and 8 GHz with *SOHO* MDI, CDS, and EIT observations. This is the first time that radio brightness temperatures as large as 10^6 K have been observed in a 15 GHz solar radio source above the limb. The field strength measurements yield a magnetic scale height L_B = 10,000 km.

Active region loops. Nagata *et al.* (2003) compared simultaneous observations of coronal loops above an active region in Fe IX, X 171 Å (formed at temperatures of 0.9 – 1.0 MK), Fe XII 195 Å (1.5 MK), and Fe XV 284 Å (2.0 – 2.5 MK) from *SOHO* EIT, Fe XIV 211 Å (1.8 MK) from the Japanese XDT sounding rocket payload, and the *Yohkoh* Soft X-ray Telescope (SXT; > 3 MK). They found that the hot loops visible in soft X-rays were distinct from the cooler loops visible in the EUV, and in general the two types of loops alternated spatially. Neither sort of loop, however, appeared to be isothermal.

An explanation for EUV "blinkers." "Blinkers," repeated intensity enhancements in transition region emission lines over, typically, 6 – 26 minutes have previously defied identification with known solar atmosphere phenomena (*e.g.* Harrison *et al.* 2003). A new study of limb events by O'Shea *et al.* (2005), however, indicates that blinkers may be macrospicular material which is repeatedly heated, but never to coronal temperatures.

Nonequilibrium in strong downflows. Lanzafame *et al.* (2005) used a large number of EUV lines to produce differential emission measures (DEMs) for regions of "quiet" Sun, and found that the DEM remains essentially the same across the quiet areas observed, except for regions with electron densities $n_e < 2 \times 10^7$ cm^{-3} and downflows > 50 km s^{-1}. The correlation of such behavior with intensity ratios from pairs of Li-like and Be-like lines that differ from those expected from ionization equilibrium calculations may indicate significant nonequilibrium in the low-density, strong-downflow regions.

EUV bright points. McIntosh and Gurman (2005) have assembled a database of over one hundred million individual EUV bright point instances from the over 360,000 EIT full-disk images over the last ten years. The database identifies which of these instances can be tracked from image to image, and therefore represent bright points with lifetimes longer than the cadence of the EIT observations. This database, which should be available for public access in the next year, is being mined for properties of EUV bright points. Figure 12 shows distributions of lifetimes obtained in this way for three different solar rotations. The distributions appear to be power laws with "knees;" that is, with an exponential component. The two components may represent distinct processes that transport or destroy

the small-scale magnetic bipoles in the lower solar atmosphere, and work is proceeding to investigate this possibility.

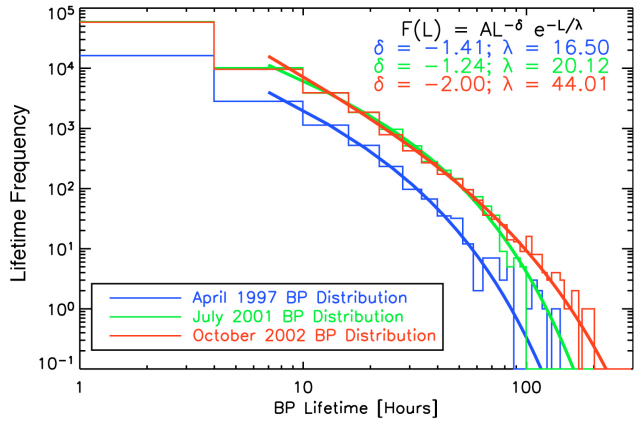

Figure 12. Lifetime distributions for coronal bright points observed in Fe XII 195 Å by SOHO EIT, derived from the 12-minute, full-resolution "CME watch" usually carried out by EIT. The 2001 July and 2002 October distributions are each the result of tracking over 200,000 individual bright points.

Loop oscillations. Marsh *et al.* (2003) observed active region loops simultaneously with *SOHO* CDS and TRACE, and were able to detect 5 minute oscillations propagating from the chromosphere and transition region into coronal loops, where they are quickly damped. The authors interpret these observations as mode conversion from slow magnetoacoustic waves to kink waves at the higher temperatures.

Coronal Mass Ejections

The three-dimensional structure of CMEs. Using relatively rare polarized brightness (pB) measurements of the corona by LASCO, Moran and Davila (2004) showed that the well-known decrease of pB with distance from the plane of the sky can be used to construct volumetric images of CME structures. Figure 13 shows such a reconstruction of an earthward-directed ("halo") CME, as seen from both north of the plane of the ecliptic and using a color table to indicate distance from the plane of the sky. Members of the LASCO PI team (Dere *et al.*2005) were able to produce similar results for later events. When combined with the additional views from the coronagraphs on the STEREO spacecraft to be launched

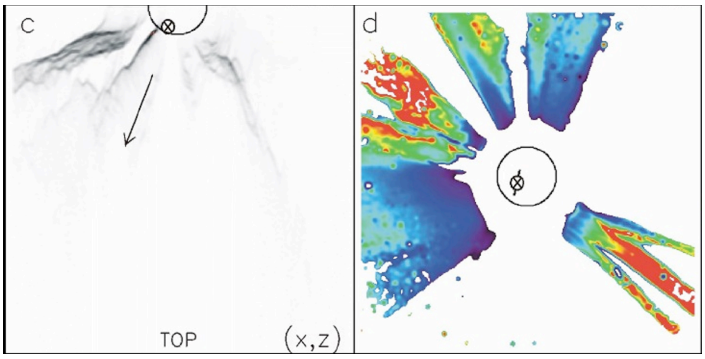

Figure 13. Reconstruction of earthward-directed CME structure from pB measurements (Moran and Davila 2004). In the left *panel, viewed from north of the ecliptic plane, the sides of the halo CME can be seen; the arrow represent the extension of the radius vector to the active region (marked by the circled X) in which the CME originates. In the* right *panel, colors represent distances from the plane of the sky, with red farthest (and thus closest to earth) and purple nearest (and thus farthest from the earth).*

in 2006, this technique should significantly reduce ambiguities in the reconstruction of interplanetary CME morphology.

Automated CME identification. Robbrecht and Berghmans (2004) have developed a means of detecting CMEs accurately in software using a Hough transform to identify appropriately sloped ridges in height-time representations of time series of coronagraph images. The method is able to capture upwards of 75% of the CMEs currently detected by (trained) eye.

Current sheets. Bemporad *et al.* (2005) have recently used *SOHO* UVCS, LASCO, and EIT and Ulysses observations when the two spacecraft were in quadrature to follow the evolution of current sheets that connect CMEs to flare loops in long duration events. During a CME on 2002 November 26, UVCS detected extended emission in the Fe XVIII 974.8 Å overlying the growing post-flare (or, more properly, post-CME) loop system beneath the CME; over the 2.3 days following the CME eruption, the electron temperature in the current sheet starts above 8×10^6 K and drops by more than a factor of two. During the same time, the current sheet density remains constant to within 10%, at about 10^8 cm^{-3}. The Ulysses SWICS instrument, meeting the interplanetary CME head-on, detected high ionization states of Fe with rapid temporal variations suggesting bursty, rather than smooth, reconnection in the coronal current sheet. This appears to indicate that not all high charge state Fe is a result of magnetic connectivity to the flaring region. The combination of remote sensing and in situ observations are consistent with the theoretical CME model by Lin & Forbes (2000) which predicts a hot current sheet that trails behind a flux rope CME. Remote sensing diagnostics of such current sheets are important as they are potential sites for the acceleration of solar energetic particles.

Lin *et al.* (2005) measured the rate at which the cool plasma at the sides of an edge-on current sheet came back together, giving the speed of reconnection in an event on 2003 November 18. They compared this to the speeds of blobs moving up the current sheet as seen by LASCO, which is expected from theory to be the Alfvén speed. Comparison of the two speeds shows that plasma enters the current sheet within the range of 0.01 to 0.23 V_A, in accord with some theoretical ideas for rapid reconnection.

Evidence for the flux rope model. Using measurements made by the NEAR magnetometer when that spacecraft was in quadrature with *SOHO*, Rust *et al.*(2005) have observed magnetic field signatures associated with a flux rope in eight of ten CMEs observed by *SOHO* LASCO that passed NEAR, and most show the expected field chirality (twist handedness) and orientation. The authors interpret these results as evidence that the flux rope believed to be visible trailing the leading edge of the CME is the flux rope sampled in interplanetary space.

Shocks and solar energetic particles. Vourlidas *et al.*(2003) used a detailed, MHD model to show that sharp-edged CMEs can be interpreted as shocks; the deflection of pre-existing streamers when impinged on by such CMEs can be seen as further evidence for white-light detection of shocks. Ciaravella et al. (2005a,b) analyzed UVCS observations of CME-driven shock waves in seven events, tripling the number of shocks observed in the UV (Ciaravella et al. 2005b). SEPs consistent with gradual acceleration in a coronal shock were detected, though the charge state measured *in situ* was below that expected from the coronal observations. In the course of analyzing this event, a new diagnostic technique, pumping of O VI 1037 Å by O VI 1032 Å and pumping of O VI 1032 Å by H Lyman β, was developed. These measurements indicate outflow speeds as high as 1800 km s^{-1} in some parts of this CME.

CME acceleration. Zhang *et al.* (2004) found that in three CMEs with very different acceleration rates, changes in the CME acceleration were correlated in time with the first derivative of the flare soft X-ray flux as measured by the NOAA GOES soft X-ray

photometers. They argue that large-scale CME acceleration and flare particle acceleration may be driven by the same physical processes.

Coronal jets. A coronal jet observed by UVCS, CDS, EIT, LASCO, and ground-based instruments crossed the UVCS observing position at 1.64 R_{Sun}, but with a speed too low to reach the UVCS position at 2.33 R_{Sun}. Ko *et al.* (2005) showed that a ballistic model explains the surprising differences between Doppler velocities measured with CDS and UVCS and also predicts dynamics and thermal properties in agreement with those observed.

The Solar Wind

Preferential Ion Heating in Coronal Holes. *SOHO* UVCS observations over the past nine years have driven new interest in collisionless wave-particle resonances, specifically the ion cyclotron resonance, as potentially important mechanisms for damping wave energy and preferentially energizing positive ions in the accelerating solar wind. One potential difficulty with this mechanism is that ion cyclotron waves – with frequencies between 10 KHz in the low corona and 1-10 Hz in interplanetary space – have not yet been observed in the corona, and are so different in frequency from the < 0.01 Hz Alfvén waves that are widely believed to be dominant.

Mechanisms that have been suggested for the generation of ion cyclotron waves in the extended corona include MHD turbulent cascade, kinetic plasma instabilities, and wave mode conversion by reflection or refraction. MHD turbulence is known to exist in interplanetary space, and much recent work has gone into trying to understand its properties in coronal plasma. Although there is strong evidence for MHD turbulence in the corona, both numerical simulations and analytic descriptions indicate that the cascade from large to small length scales occurs most efficiently for modes that do *not* become ion cyclotron resonant. In the corona, the expected type of turbulent cascade would tend to give rise to low-frequency kinetic Alfvén waves (KAWs), which damp to heat the electron T_e, not the ion T_{ion} as observed. Very recently there have been several ideas proposed to explain this apparent divergence between theory and measurement: *(a)* There could be unanticipated kinds of "frequency cascade" that arise because of the dispersive properties of the minor ions (Gomberoff et al. 2004); *(b)* if the plasma conditions in the corona become sufficiently inhomogeneous, the plasma becomes susceptible to local microinstabilities that damp the fluctuations and can lead to rapid growth of ion cyclotron waves (*e.g.* Zhang 2003; Markovskii and Hollweg 2000; Voitenko and Goossens 2004); *(c)* on the smallest spatial scales, MHD turbulence has been shown to develop into a collection of narrow current sheets undergoing oblique magnetic reconnection (*i.e.*, with the strong "guide field" remaining relatively unchanged). Dmitruk *et al.* (2004) performed test-particle simulations in a simulated turbulent plasma and found that protons can become perpendicularly accelerated around the guide field because of (cyclotron-like) coherent forcing from the perturbed fields associated with the current sheets; and *(d)* the low-frequency kinetic Alfvén waves that are believed to be generated from MHD turbulence may give rise to substantial electron beams when they damp. Sufficiently strong beamed distributions would then be unstable to the generation of parallel Langmuir waves. Evolved Langmuir wave trains exhibit a periodic electric potential-well structure in which some of the beam electrons can become trapped. Adjacent potential wells may then merge with one another and form isolated "electron phase space holes" of saturated potential. Matthaeus et al. (2003) and Cranmer and van Ballegooijen (2005) described how these tiny (Debye-scale) electrostatic structures can heat ions perpendicularly via Coulomb-like "collisions."

Origins of Fast and Slow Solar Wind. Cranmer and van Ballegooijen (2005) present a comprehensive model of how incompressible Alfven waves are generated in the photosphere, propagate up funnel-like, open flux tubes, and are linearly reflected to seed the turbulent cascade, as well as how the cascade flux determines the gross properties of coronal heating. Tu *et al.* (2005) describe SUMER observations and models that support the view of solar wind acceleration in funnel-like flux tubes originating in coronal holes, and isolate the source region for the acceleration of the wind to between 5 and 20 Mm above the solar surface. Paradoxically, McIntosh and Leamon (2005), using MDI photospheric magnetic field measurements and determinations of the sound travel time between the heights of formation of two chromospheric continua observed with TRACE, find that the sound travel time over different magnetic features (low-latitude coronal holes and active regions) predicted not only the wind speed observed by ACE but the wind composition as well. Why the chromosphere should "know" about the solar wind above it is not yet clear, but the open and closed magnetic geometries have very different gas pressure scale heights. Other recent studies focus on the self-consistent computation of solar wind models using a relatively simple Kolmogorov version of the turbulent damping (Li 2003).

Vasquez *et al.* (2003) and Cranmer (2005) have studied the differences between fast and slow wind at solar minimum as an effect of the different rates of superradial flux-tube expansion over the polar coronal holes and at the edge of the streamer belt. A combination of two effects is able to produce the observed differences: a raising of the height of the Parker critical point for flux tubes within about 20 degrees of the closed-field part of the streamer tends to produce a slow wind solution; and the near-streamer flux tubes undergo a lower rate of Alfvén wave dissipation at heights at and above the critical point, which leads to a lower wind speed and higher mass loss rate.

Observationally, there is growing evidence that coronal holes and streamers share at least some of the same microphysical processes. Frazin *et al.* (2003) found a significantly higher kinetic temperature for O VI than for H above 2.6 solar radii in an equatorial solar-minimum streamer, and that O VI exhibits an anisotropic velocity distribution with $T_{ion} > T_e$ (see also Strachan *et al.* 2004). Miralles *et al.* (2004) showed that solar-minimum streamers fall naturally along the same empirical sequence of velocity/temperature parameter space as a collection of dozens of large polar coronal holes that occurred over the last solar cycle. These two observations indicate that ion cyclotron resonance may be operating in both coronal holes and streamers, and that the onset of preferential ion heating may be modulated by density.

Solar wind composition

HIDEs. Solar wind composition is known to vary modestly as a function of First Ionization Potential, as well as in different solar wind flow types (*e.g.* the low speed interstream wind, coronal hole associated wind, CMEs). The *SOHO* CELIAS MTOF group (at the University of Maryland), however, has recently identified a new type of event. In these Heavy Ion Depletion Events (HIDEs), He and all the heavier ions are depressed relative to solar wind protons by one to two orders of magnitude. Figure 14 shows the behavior of protons and alpha particles in one such event. The He density derived from both ACE and *SOHO* instruments are in good agreement and demonstrate the ratio He/H decreases from its nominal value of ~ 0.04 to ~ 0.001. This factor of ~ 40 decrease is also observed in the ratios of O/H and Fe/H.

Using both *SOHO* MTOF and ACE SWICS data, six such events (with durations ranging from ~ 6 to 48 hours) have been identified. At least three of these HIDEs occur in the declining phase of high speed streams. A possible explanation for these events is based on the model by Fisk (1996), in which differential rotation produces a merging of open coronal hole field lines with old, closed field lines in the equatorial region. These old, closed field lines are thought to be depressed in heavy ions due to gravitational settling. Evidence for such gravitational settling has been reported in quiescent streamers by *SOHO*/UVCS (e.g., Raymond 1999).

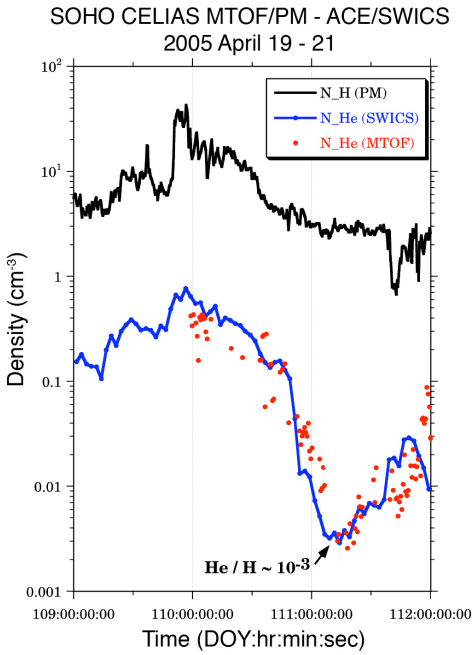

Figure 14. Proton (black: *SOHO CELIAS MTOF proton monitor) and helium* (blue: *ACE SWICS*, red: *SOHO CELIAS MTOF) densities during the Heavy on Depletion Event of 2005 April 19 – 21.*

Solar Energetic Particles

Energy Dependent Charge States in Impulsive Events. The ionic charge distributions of solar energetic particles (SEP) are an important diagnostic of the plasma conditions of the source region in the solar corona. Furthermore, acceleration and transport processes depend significantly on velocity and rigidity, *i.e.*, on the mass and charge of the ions. In the past, SEP events were grouped into two classes, so-called gradual and impulsive events, where the particles in impulsive events originate in the flare region and those in gradual events, at least up to energies of a few Mev/nuc, are predominantly accelerated at coronal and/or interplanetary (IP) shocks. Because of the large differences between the mean ionic charge of Fe in the MeV/nuc energy range in events identified as gradual (Q(Fe)~14) and impulsive (Q(Fe) ~20), the ionic charge states were also used as a defining characteristic for this classification.

New measurements of ionic charge states with instruments of improved sensitivity over a wide energy range on several spacecraft (SAMPEX, *SOHO*, ACE), however, have shown that this picture was oversimplified. In IP-shock related events, the ionic charge state of heavy ions was observed to generally increase with energy, with a large event to event variability. For impulsive events, previous work indicated a systematic but modest

increase of Q(Fe) with energy in the range 180-550 keV/nuc. However, measurements with *SOHO* CELIAS STOF now show (Figure 15) that the ionic charge of Fe at energies < 100 keV/nuc in these events is significantly smaller (~12.5±0.9). The large increase of the mean ionic charge of iron in the energy range ~10-550 keV/nuc as observed with *SOHO* and ACE can only be explained in terms of impact ionization by protons and electrons in a dense environment in the low corona, at altitudes < 2 R_{Sun}.

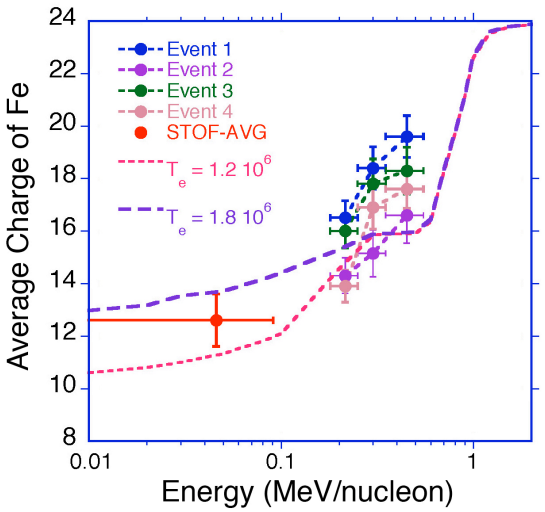

Figure 15. Charge states of Fe as a function of energy as taken with SOHO CELIAS STOF and ACE SEPICA for several impulsive events together with energy dependence obtained for equilibrium conditions in a charge stripping model, from Klecker et al. (2005).

The interplanetary highway. *SOHO* ERNE has continued to conduct precise observations of solar energetic particles (SEPs) associated with solar flares and coronal mass ejections (CMEs), focusing on exceptionally accurate measurements of the proton flux anisotropy (Figure 16). These measurements have made possible the discovery of an interplanetary "highway" for solar energetic particles. ERNE measured the proton flux anisotropy during the 1998 May 2-3 SEP event, when *SOHO* was inside a magnetic cloud associated with a previous CME. During most of the first four hours of the SEP event the proton intensity parallel to the magnetic field was ~1000 times higher than in the perpendicular direction. The ERNE observations (Torsti et al. 2004) indicate that the magnetic flux-rope structure of the CME provides a "highway" for transport of solar energetic protons with a parallel mean free path of at least 10 AU. The SEP anisotropy observed in the solar wind at 1 AU may be related to processes of solar wind acceleration, because those processes also load the solar wind with the turbulence that scatters SEPs. There is increasing evidence that acceleration of the normal solar wind is a result of the reconnection of open magnetic flux with coronal loops. If so, these observations may indicate that the closed flux of the magnetic rope has experienced far fewer reconnections than the open flux of the quiet solar wind, and for this reason there are fewer small-scale irregularities within CMEs from which to scatter high-energy protons.

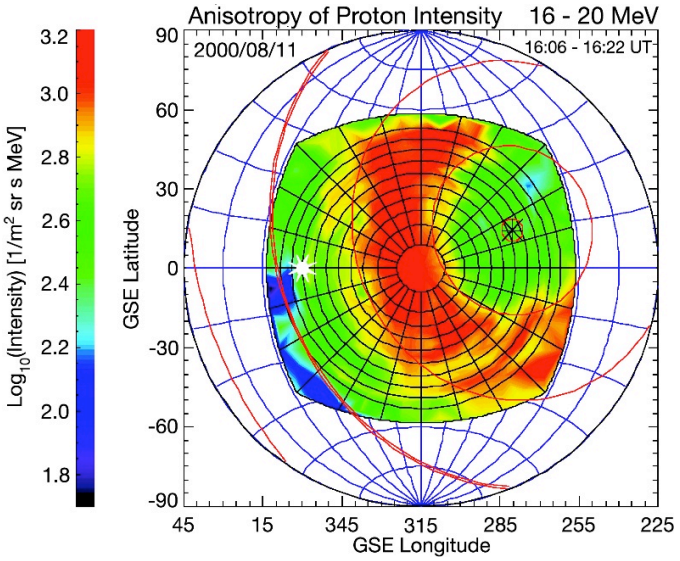

Figure 16. Illustration of exceptionally precise observations of the high-energy particle telescope ERNE/HED: Unusual loss-cone angular distribution of high-energy protons observed with ERNE approximately two hours before the arrival of the interplanetary CME-driven shock on August 11, 2000. Magnetic field direction is shown with black asterisk; directions perpendicular to the magnetic field are mapped with the red double curve; white asterisk shows the Sun.

Common overabundance of high-energy ^{3}He. Torsti *et al.*(2003) used a survey of ERNE energetic particle measurements for the period of 22 months from 1999 February 8 to 2000 December 7 to study the regularities of ^{3}He enhancements in high-energy range of 15-30 MeV nucleon^{-1}. The statistical study revealed details challenging traditional impulsive-gradual paradigm of solar energetic particle events.

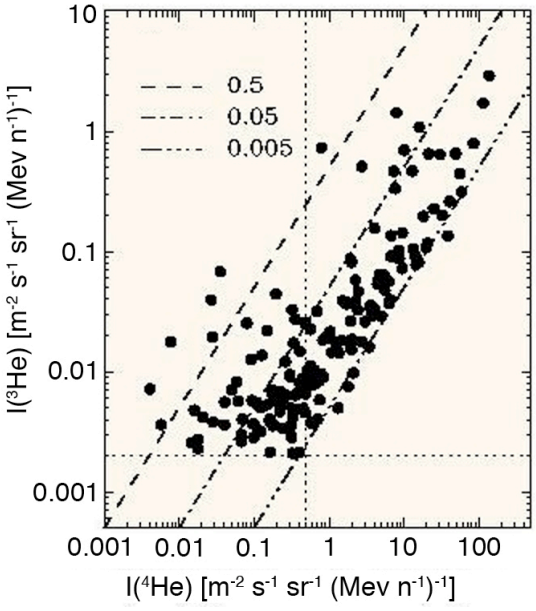

Figure 17. Scatter plot of ^{3}He intensity vs. ^{4}He intensity, with background subtracted, on ^{3}He event days in energy channel 15-30 MeV nucleon^{-1}. The horizontal dotted line exemplifies an average ^{3}He background level. All ^{4}He enhancements with ^{4}He intensity exceeding the threshold level shown by the vertical line are associated with measurable ^{3}He.

Figure 17 shows the daily average ^{3}He intensities versus the ^{4}He intensities on the ^{3}He

event days with galactic background reduced. In the scatter plot a clear correlation between ^{3}He and ^{4}He intensities can be seen. Most of the events are located between ^{3}He/^{4}He ratio lines 0.005 and 0.05, especially in strong events. The survey revealed also that significant fluxes of ^{3}He ions have been detected in all ^{4}He events with intensity exceeding value I(^{4}He) ≈ 0.5 ions of ^{4}He per (m^2 s sr MeV nucleon^{-1}). Figure 18 shows a statistical distribution of the ^{3}He enhancement days *versus* the ^{3}He/^{4}He ratio. The distribution apparently consists of a narrow peak at ^{3}He/^{4}He ~ 0.01 and wide substratum extending through ^{3}He/^{4}He ~1. The widely quoted "normal" abundance ratio ^{3}He/^{4}He ≈ 5 x 10^{-4} finds no support in the observations in this energy range.

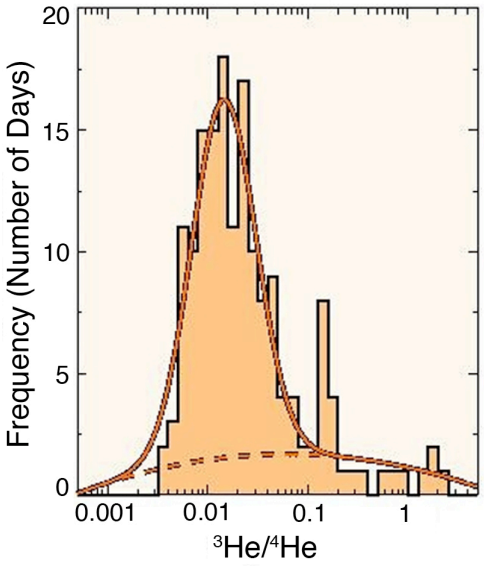

Figure 18. The distribution of ^{3}He event days over the abundance ratio ^{3}He/^{4}He. The red lines represent a possible fit to the data histogram. Distribution reveals a main peak around ^{3}He/^{4}He = 0.01 and a high-abundance tail at ^{3}He/^{4}He > 0.1.

The Heliosphere and Beyond

He II in the heliosphere. Spatial variations in helium photoionization rates due to the anisotropy of solar EUV emission significantly affects the determinations of interstellar He density from *Ulysses* GAS measurements. Using EIT 304 Å images and an accurate differential emission measure (DEM) model that makes it possible to isolate only those features in the images produced by He II emission, Auchere *et al.* (2005) have been able to construct all-sky maps of He II flux at arbitrary distances up to 1 AU; these should be useful in correcting the interstellar He densities.

Solar wind anisotropies. Over the first half of the current solar cycle (1995 – 2001), SWAN measurements (Lallement *et al.* 2004) show that the solar wind mass flux at high latitudes increases by nearly a factor of two, as the polar coronal holes disappear in the rise to solar maximum. Bzowski *et al.* (2003) interpret a north-south asymmetry in the mass flux as being driven by the solar dynamo, rather than a signal difference caused by different photoionization rates in the northern and southern hemispheres.

An interstellar compass. Lallement *et al.* (2005) have used SWAN H cell measurements to determine that the direction of the interstellar hydrogen flow differs by 4.0°±0.5° from that of the interstellar helium; this in turn leads to a determination of the direction of the magnetic field in the local interstellar medium. Izmodenov *et al.* (2005) employ a 3-D,

kinetic, MHD model of solar wind interaction with the magnetized, interstellar plasma to explain the measured deviation; to do so, their model requires that the insterstellar magnetic field have a magnitude of ~ 2.5 μG and an inclination of 45^o to the direction of interstellar flow.

References

Antia, H.M. and Basu, S., 2005, *Astrophysical Journal*, 620, L129

Antiochos, S.K. Devore, C.R., and Klimchuk, J.A. 1999, *ApJ*, 510, 485

Asplund, M., Grevesse, N., Sauval, A.J., Allende Prieto, C., and Kiselman, D. 2004, *Astronomy and Astrophysics,* 417, 751-768

Asplund, M., Grevesse, N., Sauval, A.J., and Lodders, K., 2005a, *ASP Conf. Ser. 336: Cosmic Abundances as Records of Stellar Evolution and Nucleosynthesis Meteoritics & Planetary Science, 38, Supplement, abstract no.5272,* 336 38: p.25

Asplund, M., Grevesse, N., and Sauval, A.J. 2005b, *ASP Conf. Ser. 336: Cosmic Abundances as Records of Stellar Evolution and Nucleosynthesis*, 38, p. 25

Auchère, F. Cook, J.W., Newmark, J.S., McMullin, D.R., von Steiger, R., and White, M. 2005, *ApJ*, 625, 1036

Bahcall, J.N. and Serenelli, A.M., 2005, *Astrophysical Journal,* 626, 530

Bahcall, J.N., Basu, S., Pinsonneault, M., and Serenelli, A.M., 2005, *Astrophysical Journal,* 618, 1049

Bemporad, A., Poletto, G., Suess, S. T., Ko, Y.-K., Schwadron, N. A., Elliot, H.A., & Raymond, J.C. 2005, submitted to *ApJ*

Benevolenskaya, E.E., 2003, *Solar Physics,* 216, 325

Bothmer, V. and Schwenn, R. 1998, *Ann. Geophysicae*, 16, 1

Bothmer, V. 2003, in *Solar variability as an input to the Earth's environment: International Solar Cycle Studies (ISCS) Symposium*, A. Wilson, ed., p. 419

Brosius, J.W. and White, S.M. 2005, submitted to Ap.J.

Brown, B.P., Haber, D.A., Hindman, B.W., and Toomre, J. 2004, in *ESA SP-559: SOHO 14 Helio- and Asteroseismology: Towards a Golden Future*, p. 345

Bzowski, M., Mäkinen, T., Kyrölä, E, Summanen, T. Quémerais, E. 2003, A&A, 408, 1165

Chané, E., C. Jacobs, B. van der Holst, Poedts, S., and Kimpe, D. 2005, *A&A*, 432, 331

Ciaravella, A., Raymond, J.C., Kahler, S.W., Vourlidas, A. & Li, J. 2005b, ApJ, 621, 1121

Ciaravella, A., Raymond, J.C. & Kahler, S.W. 2005a, ApJ, submitted

Couvidat, S., García, R. A., Turck-Chièze, S., Corbard, T., Henney, C. J., Jiménez-Reyes, S. 2003, *Ap.J.*, 597, L77

Cranmer, S. R. 2005, in Solar Wind 11/*SOHO*-16: Connecting Sun and Heliosphere, ESA SP-592, in press, *arXiv astro-ph/0506508*

Cranmer, S. R., van Ballegooijen, A. A., 2003, *ApJ*, 594, 573

Cranmer, S. R., van Ballegooijen, A. A., 2005, *ApJ Suppl.*, 156, 265

Dere, K.P., Wang, D., and Howard, R.A. 2005, *ApJ*, 620, L119

Dikpati, M., de Toma, G., Gilman, P.A., Corbard, T., Rhodes, E.J., Haber, D.A., Bogart, R.S., and Rose, P.J., 2004, *Bull. AAS,* 204, 5305

Dmitruk, P., Matthaeus, W. H., Seenu, N. 2004, *ApJ*, 617, 667

Donea, A.-C. and Lindsey, C. 2005, *Ap.J.*, 630, 1168

Dziembowski, W.A. and Goode, P.R., 2004, *Astrophysical Journal,* 600, 464

Dziembowski, W.A. and Goode, P.R., 2005, *Astrophysical Journal,* 625, 548

Dzifcakova, E., Kulinova, A., and Kosovichev, A.G. 2003, in *ESA SP-517: GONG+ 2002. Local and Global Helioseismology: the Present and Future*, p. 263

Fisk, L. A. 1996, *JGR*, 101, 15547

Foukal, P., North, G., Wigley, T, 2004, *Science,* 306 (5693), 68

Fröhlich, C. 2006, *Space Sci. Rev.*, in press

Frazin, R. A., Cranmer, S. R., Kohl, J. L., 2003, *ApJ*, 597, 1145

Gomberoff, L., Munoz, V., Valdivia, J. A. 2004, *Plan. Space Sci.*, 52, 679

Guzik, J.A., Watson, L.S., and Cox, A.N., 2005, *Astrophysical Journal,* 627, 1049

Haber, D.A., 2003. in *Solar and Solar-Like Oscillations: Insights and Challenges for the Sun and Stars, 25th meeting of the IAU, Joint Discussion 12, 18 July 2003, Sydney, Australia,* 12: p. 44

Haber, D.A., Hindman, B.W., Toomre, J., Bogart, R.S., Larsen, R.M., and Hill, F., 2002, *Astrophysical Journal,* 570, 855

Haber, D.A. 2004, in *ESA SP-559: SOHO 14 Helio- and Asteroseismology: Towards a Golden Future*, p. 676

Harrison, R.A., Harra, L.K., Brkovic, A., and Parnell, C.E. 2003, *A&A*, 409, 755

Hindman, B.W., Gizon, L., Duvall, T.L., Jr., Haber, D.A., and Toomre, J., 2004a, *Astrophysical Journal,* 613,1253
Hindman, B.W., Featherstone, N.A., Haber, D.A., Musman, S., and Toomre, J. 2004b, in *ESA SP-559: SOHO 14 Helio- and Asteroseismology: Towards a Golden Future*, p. 460
Hollweg, J.V. 2000, *JGR*, 105, 15699
Howe, R., Komm, R.W., Hill, F., Christensen-Dalsgaard, J., Haber, D.A., Schou, J., and Thompson, M.J. 2004, in *ESA SP-559: SOHO 14 Helio- and Asteroseismology: Towards a Golden Future*, p. 472
Izmodenov, V.; Alexashov, D.; Myasnikov, A.2005, A&A, 437, L35
Klecker, B., Möbius, E., Popecki, M., Kistler, L.M., Kucharek, H. and Hilchenbach, M. 2005, Adv. Space Res., in press
Ko, Y.-K., *et al.* 2005, *ApJ*, 623, 519
Kocharov, L., Kovaltsov, G. A., Torsti, J., and Huttunen-Heikinmaa, K. 2005, *JGR - Space Physics*, in press
Komm, R., Howe, R., González Hernández, I., Hill, F., Sudol, J., and Toner, C. 2004, in *ESA SP-559: SOHO 14 Helio- and Asteroseismology: Towards a Golden Future*, p. 158
Kosovichev, A.G. 2005, in preparation
Kosovichev, A.G. and Duvall, T.L., Jr. 2003, in *Innovative Telescopes and Instrumentation for Solar Astrophysics.* Keil, S. and Avakyan, S. eds., *Proceedings of the SPIE,* 4853, 327
Kosovichev, A.G. and Zharkova, V.V. 1998, *Nature,* 393, 317
Kulinova, A., Dzifcakova, E., Duvall, T.L., Jr., and Kosovichev, A.G. 2003, in *ESA SP-535: Solar Variability as an Input to the Earth's Environment*. p. 125
Lallement, R., Raymond, J.R., and Vallerga, J. 2004, Adv. Space Res., 34, 46
Lallement R., Quémerais E., Bertaux J.L., Koutroumpa D., Ferron S., Pellinen R. 2005, Science, 307 (5714), 1447
Lanzafame, A., Brooks, D.H., and Lang, J. 2005, *A&A*, 432, 1063
Lefebvre, S., and Kosovichev, A.G., 2005, *Ap. J. Letters,* submitted
Li, X. 2003, *A&A*, 406, 345
Lin, J. & Forbes, T. G. 2000, *JGR*, 105, 2375
Lin, J., Ko, Y.-K., Sui, L., Raymond, J.C., Stenborg, G.A., Jiang,Y., Zhao, S., and S. Mancuso, S., 2005, *ApJ*, 622, 1251
Lodders, K., 2003, *Meteoritics & Planetary Science, vol. 38, Supplement,* 38, 5272
Marsh, M.S., Wlash, R.W., DeMoortel, I., and Ireland, J. 2003, A&A, 404, L37
Markovskii, S. A., Hollweg, J. V. 2004, *ApJ*, 609, 1112
Matthaeus, W. H., Mullan, D., Dmitruk, P., Milano, L., Oughton, S. 2003, *Nonlin. Proc. Geophys.*, 10, 93
Miralles, M. P., Cranmer, S. R., Kohl, J. L. 2004, *Adv. Space Res.*, 33 (5), 696
McIntosh, S.W. and Gurman, J.B. 2005, *Solar Phys.*, 228, 285
McIntosh, S.W. and Leamon, R.J. 2005, Ap.J., 624, L117
Moran, T.G. and Davila, J.M. 2004, *Science*, 305, 66
Nagata, S. *et al.* 2003, *ApJ*, 590, 1095
O'Shea, E., Banerjee, D., & Doyle, J.G. 2005, *A&A*, 436, L43
Raymond, J.C. 1999, *Space Sci. Rev.*, 87, 55
Raymond, J.C. and Ciaravella, A. 2004, *ApJ*, 606, L159
Robbrecht, E. and Berghmans, D. 2004, *A&A*, 425, 1097
Rust, D.M., Anderson, B.J., Andrews, M.D., Acuña, M.H., Russell, C.T., Shuck, P.W., and Mulligan, T. 2005, ApJ, 621, 524
Strachan, L., Baham, M., Miralles, M. P., Panasyuk, A. V. 2004, in *SOHO*-15: Coronal Heating, eds. R. W. Walsh, J. Ireland, D. Danesy, B. Fleck, ESA SP-575, 148
Thernisien, A.F., Morrill, J.S., Howard, R.A., and Wang, D. 2005, *Solar Physics*, in press
Torsti, J., Laivola, J., and Kocharov, L. 2003, *A & A*, 408, L1
Torsti, J., Riihonen, E., and Kocharov, L. 2004, A*pJ*, 600, L83
Tu, C.-Y., Zhou, C., Marsch, E., Wilhelm, K., Zaho, L., Xia, L.-D., Wang, J.-X., 2005, *Science*, 308, 519
Turck-Chièze, S., Couvidat, S., Piau, L., Ferguson, J., Lambert, P., Ballot, J., García, R.A., and Nghiem, P., 2004, *Physical Review Letters*, 93, 211102
Turck-Chièze, S. *et al.* 2004, *Ap.J.*, 604, 455
Vasquez, A. M., et al., 2003, *ApJ*, 598, 1361
Voitenko, Y., Goossens, M. 2004, *ApJ*, 605, L149
Vourlidas, A. Wu, S.T., Wang, A.H., Subramanian, P., and Howard, R.A. 2003, *ApJ*, 598, 1392
Zhang, J. Dere, K.P., Howard, R.A., and Vourlidas, A. 2004, *ApJ*, 604, 420
Zhang, T. X. 2003, *Ap.J.*, 597, L69
Zhao, J. and Kosovichev, A.G. 2004a, in *ESA SP-559: SOHO 14 Helio- and Asteroseismology: Towards a Golden Future*, p. 67
Zhao, J. and Kosovichev, A.G., 2004b, *Astrophysical Journal,* 603, 776

IV. *SOHO* Scientific Objectives, 2006 - 2010

The NASA Sun-Solar System Connection (S3C) 2005 – 2035 Science and Technology Roadmap takes as its current paradigm the "distributed network of spacecraft we call the [S3C] Great Observatory" because of the rich variety of physically connected phenomena those spacecraft were able to observe during the period 2003 October 19 – November 5. Take away any part of the network – remote sensing of the Sun, the heliosphere, the terrestrial magnetosphere, ionosphere, and thermosphere; *in situ* measurements of plasma parameters, energetic particles, and magnetic field from a variety of vantage points; or the data and modeling systems that enable access to and analysis of so much data – and the entire network collapses. Budgetary constraints usually prevent much redundancy in the Great Observatory assets in space, and the next five years should see a unique expansion of the observing capabilities of the network, if we can continue to provide the only "pacing consumable" of most of our S3C missions: budget.

The planned launches of STEREO and Solar-B in 2006, and of the Solar Dynamics Observatory (SDO) in 2008 will make possible new and important observations that will address the Roadmap questions ("research focus areas/investigations") F2.1 (How are charged particles accelerated to high energies?), F2.3 (How is the solar wind accelerated and how does it evolve?), F3.4 (How do the heliosphere and interstellar medium interact?), F4.1 (How do subsurface flows drive the solar dynamo and produce the solar cycle?), F4.2 (How are open flux regions produced on the Sun, and how do variations in open flux topology and magnitude affect heliospheric structure?), H1.1 (How do solar wind disturbances propagate and evolve from the Sun to the earth?), H1.2 (What are the precursors to solar disturbances, and how can we predict solar disturbances that impact Earth?), H3.3 (How do long term variations in solar energy output affect Earth's climate?), J1.2 (How does the radiation environment vary as a function of time and position, and how should it be sampled to provide situational awareness for future human explorers?), J2.1 (What are the observational precursors and magnetic configurations that lead to CMEs and other solar disturbances, and what determines their magnitude and energetic particle output?), J2.2 (What heliospheric observations

Roadmap Investigation	*SOHO* + STEREO	*SOHO* + Solar-B	*SOHO* +SDO	*SOHO* – unique	*SOHO* + existing GO	*SOHO* +other assets
F2.1						
F2.3						
F3.4						
F4.1				SDO		
F4.2					Ulysses	
H1.1						
H1.2				SDO		
H3.3				Picard		SORCE
J1.2						
J2.1						
J2.2						
J3.1						
J3.2						
Operational information						

Table 1. Unique opportunities for new or improved science, or operational space weather information; made possible by SOHO collaborations with: missions to be launched in FY06 – FY08; other, existing Great Observatory missions; other on-orbit assets; and uniquely from SOHO. Blue *areas indicate opportunities for significant new knowledge or improvement of existing understanding;* grey *areas, less significant improvements; and the* diagonally hatched *area, an opportunity of limited duration.* Green *areas indicate areas where SOHO should be superseded, c. 2009, but intercalibration will be necessary.*

and empirical models are needed to enhance the predictive capability required by future human and robotic explorers?), J3.1 (How are solar energetic particles created and how do they evolve from their coronal source regions into interplanetary space?), and J3.2 (How do solar magnetic fields and solar wind plasma connect to the inner heliosphere and what is the nature of the near-Sun solar wind through which solar disturbances propagate?). We summarize the unique opportunities for addressing these questions in Table 1, which highlights both opportunities afforded by the combination of *SOHO* observations and those from new missions, and those uniquely enabled by *SOHO*.

None of these investigations differs dramatically from the original scientific objectives of *SOHO*: to probe the solar interior and measure solar irradiance accurately; to provide better understanding of the structure, dynamics, and evolution of the outer solar atmosphere; and to study the acceleration and composition of the both the solar wind and solar energetic particles. Given the large number of new and enhanced opportunities, we have room to discuss only a few, but they give an excellent indication of the new and continuing opportunities for improved understanding of the Sun-heliosphere system and the flow of operational-quality information that combining data from *SOHO* and the newer observatories will allow.

Subsurface solar weather (F4.1, H1.2). Until the launch of SDO in late 2008, only *SOHO* MDI will be capable of producing the "subsurface solar weather" flow maps and observations of emerging magnetic flux below the photosphere (see pp. 6-7) that are at the frontier of our understanding of the magnetic variability that leads to space weather, as well as the solar cycle variations of active region-scale flux emergence.

Quadrature observations (F4.2). The extended quadrature opportunities with Ulysses in 2006 December – 2007 May (at angular separations of $90^o \pm 5^o$) and 2007 December – 2008 May ($90^o \pm 10^o$), will provide "ground-truth" measurements of the interplanetary conditions that *SOHO* will observe to 30 R_{Sun}, while Ulysses is at heliographic latitudes of 60^o or more, where the magnetic field should be rooted in the solar polar coronal holes. Models from the Community Coordinated Modeling Center (CCMC) will be able to use MDI photospheric magnetic field observations to generate predictions of the electron density structure in the corona and at 1 AU. Observations by LASCO and Ulysses – and the two STEREO spacecraft – can then be compared to the predictions, which promises to improve the MHD models.

Acceleration of the solar wind (F2.3). Several Great Observatory measurements address this critical question, but only *SOHO* UVCS and SUMER are able to monitor ion outflow speeds in the solar corona spectroscopically. Only SUMER can measure ion flow speeds at the coronal base and the initial acceleration, and only UVCS can measure supersonic outflow speeds in coronal holes and streamers, as well as highly anisotropic velocity distributions, which provide strong evidence for heating and acceleration by ion cyclotron waves. Cyclotron resonance models depend crucially on the magnitude and sign of the ion temperature gradient (Hollweg 2000), and only newly optimized UVCS observations can determine the gradient. We propose to continue SUMER and UVCS measurements in combination with high resolution *Solar-B* measurements to work toward a quantitative, predictive understanding of the solar wind.

CMEs, current sheets, and shocks (J2.1, J2.2, J3.1, J3.2). We need better characterizations of the source regions of heliospheric disturbances. Are all, or even most, CMEs characterized by the Lin and Forbes (2000)-like geometry observed by UVCS? We will pursue LASCO, EIT, UVCS, ERNE, and CELIAS observations of CMEs and energetic particle, including sufficient observations of quiescent conditions to allow the establishment of baseline conditions, consonant with the 0.2 – 0.3 CME day^{-1} rate around solar minimum, to address such questions as: *(1)* Do current sheets trailing CMEs vary with solar cycle phase, *e.g.* by lower maximum temperature or different cooling rates? *(2)* Are low-density "bubbles" in CMEs common enough to call into question the breakout model

(Antiochos *et al.* 1999)? *(3)* How do the large-scale, polar crown filament (PCF)-related events of solar minimum differ from those at solar maximum, which typically originate in active regions? *(4)* How do solar minimum and solar maximum CMEs differ in particle acceleration efficiency? (5) What is the ratio of suprathermal seed particle population to the thermal population in the corona? (The UVCS Ly α detector can be used to search for signatures of the seed population 2 – 3 Å from line center.) All of these studies will be enhanced by the analysis of events observed by STEREO as well as *SOHO*, particularly by the STEREO *in situ* and SWAVES experiments. As events in the first two weeks of 2005 September have shown, fast CMEs can occur even late in a solar cycle, and the development of "Doppler pumping" diagnostics by Raymond and Ciaravella (2004) allows the characterization of plasma moving at up to ~ 2,000 km s^{-1} with UVCS.

Dependence of CME propagation on solar cycle phase (H1.2, J2.1, J2.2). Bothmer and Schwenn (1998) related the structure of magnetic clouds in interplanetary space to the hemispheric pattern of helicity in filament channels on the Sun (predominantly left-handed twist in the northern hemisphere and right-handed twist in the southern hemisphere, for both even and odd-numbered cycles). Data from *SOHO*, *Yohkoh*, TRACE, WIND, and ACE validated these predictions (Bothmer 2003). Numerical simulations by Chané *et al.* (2005) show that the evolution of a CME is strongly influenced by the magnetic field structure of the erupting flux rope, and the structure of the ambient heliospheric magnetic field that is compressed ahead of a fast CME differs from one cycle to the next. We propose to extend our observations of CMEs and their source regions into the next cycle, including the period when magnetic flux from both old and new cycles is present in the next few years. This should lead to better understanding of how to predict geoeffectiveness as a function of CME parameters and cycle phase.

Reconstruction of CME morphology (H1.2, J2.1). One of the principal, new areas of investigation that STEREO SECCHI will enable is the tomographic reconstruction of CME morphology. The SECCHI Principal Investigator team has performed reconstructions of simulated CMEs using both two and three viewpoints in the ecliptic plane. The addition of a third viewpoint – *SOHO*'s – can eliminate a critical ambiguity in determining the total amount of material in a CME. The SECCHI PI team "consider[s] the third *SOHO* viewpoint to be critical in obtaining meaningful reconstructions using tomography, and indeed for other reconstruction techniques (forward modeling parameterized solutions, for example) also." (Of course, a viewpoint well out of the ecliptic would provide an even more dramatic improvement over two-spacecraft tomography, but none is on offer before the ESA Solar Orbiter epoch, some eleven years hence.) We therefore propose to support STEREO CME tomography efforts by continuing to provide the "third eye" for white-light coronagraphy. Similarly, we propose to continue CDS CME watch campaigns that provide the only current measurements of the speed of plasma erupting from the disk at temperatures up to 2.5 $x10^6$ K.

Multipoint SEP sampling (F2.1). The combination of the STEREO IMPACT/PLASTIC instrumentation, ACE, and *SOHO* ERNE and CELIAS STOF provides yet another novel opportunity: measuring the composition and energy spectra of energetic particle events from multiple locations, which should narrow the range of acceleration geometries.

Precursors to CMEs (H1.2). Currently, only the combination of the *SOHO* LASCO synoptic and EIT CME watch programs provide the full solar hemisphere coverage necessary to allow the detection of precursor events to coronal mass ejections, since the field of view of TRACE is simply too small to encompass all the events involved in an event as large as a CME. STEREO will significantly expand this program, both with better EUV spatial resolution and with at least one more waveband of CME watch imaging, but the STEREO spacecraft will be poorly located for observing many of the precursors of earthward-directed events some two years after launch. Solar EUV imaging will improve dramatically with the Solar Dynamics Observatory (SDO) Advanced

Imaging Array (AIA), although the LASCO coronagraphs will still be unique in years after SDO launch, currently scheduled for late 2008.

Reconstruction of EUV loop morphology (H1.2, J2.1). The STEREO SECCHI EUV Imagers (EUVIs) will be used to reconstruct the 3-D morphology of loop systems over the entire disk, but can do so only over a narrow range of spacecraft separations early in the mission: as the spacecraft separate, the area of overlap decreases, and ambiguities brought on by the optically thin nature of the EUV emission increase as multiple features begin to fall along the same line of sight for one spacecraft or the other. The addition of a third viewpoint, that of *SOHO* EIT, will double the length of time over which such reconstructions are possible.

Solar "forcing" of terrestrial climate (H3.3). A long-term, accurate, absolutely calibrated record of total solar irradiance (TSI) is essential for answering questions about the degree to which solar forcing affects climate on earth. The 26-year record of TSI (see Section III, below) will be extended when *SOHO* overlaps with the French *Picard* mission (scheduled for launch about the same time as SDO in 2008), which will carry an identical suite of radiometers to that in *SOHO* VIRGO. The absolute accuracy is still a matter of some controversy, as the SORCE TIM measurements differ from those in the NIMBUS-ACRIM-VIRGO record by some 5 W m^{-2}. The irradiance community plans to calibrate the remaining laboratory spares of TIM, VIRGO PM06V and DIARAD, and ACRIM-III against cryogenic radiometers at NIST and JPL to remove this remaining ambiguity.

Heliospheric interactions with the interstellar medium (F3.4). It is not just the plasma and neutral gas in the heliosphere and the interplanetary medium that interact: interplanetary H Lyman α is resonantly scattered by solar wind protons, and full-sky observations can provide us with information on the motion of the heliosphere relative to the local interplanetary medium, and even the direction and magnitude of the magnetic field at the "front" of the heliosphere (cf. pp. 20-21). In the Great Observatory, currently only *SOHO* SWAN obtains such measurements.

Space weather early warning

Although the NOAA Space Environment Center (SEC) is responsible for predicting space weather in geospace, they have disclaimed any role in forecasting space weather elsewhere in the solar system. For the Exploration effort, therefore, NASA will have to provide its own space weather information.

Operational information on CME speeds and directions. While STEREO will inaugurate a new era of CME characterization as its two spacecraft gradually separate, the "space weather beacon" (SWX) information from the STEREO spacecraft, with greatly reduced spatial resolution of information from the imaging instrument (SECCHI) and 12 – 24 hour delays in receipt and reformatting of full-resolution telemetry indicate that *SOHO* LASCO and EIT, with a realtime contact coverage of ~ 50% throughout the year, and delays of < 10 hours in receipt and reformatting of playback data from gaps in realtime coverage, will continue to be the primary source of operational information on the location of origin, speed, and heading of coronal mass ejections from the earth-facing hemisphere of the Sun. Even with automated detection of events in the SWX data stream, it may be difficult to confirm propagation speeds in a timely fashion for use in formulating space weather forecast information, particularly for faster CME's. In addition, after two years, the angular separation of the STEREO spacecraft will be ~ 90^{o}, and the proportion of earthward-directed events well observed by both spacecraft will begin to decrease.

L1 solar wind monitoring under extreme conditions. As noted in the 2003 Senior Review proposal, during extended SEP events, the solar wind plasma information from ACE, the primary

operational source of L1 solar wind and energetic particle information, can be become unreliable. Measurements from the *SOHO* CELIAS MTOF proton monitor are much less prone to such effects, as shown during the paradigmatic SEP storm of 2003 October 28 - 29. These will be carried out as long as *SOHO* is operational.

Discovery science. As the National Academy's Space Studies Board said in its review of the S3C Roadmap, "fundamental discovery science" may be undervalued in the Roadmap because of the previous NASA administration's focus on a "utilitarian" approach to science. The current NASA administration appears to view science as a part of Exploration, and as the next section testifies, *SOHO* PI team members, Guest Investigators, and our colleagues in the worldwide solar and heliospheric physics community will continue to make discoveries as they have over the past decade of *SOHO* observations.

V. Technical and Budget, FY06 – FY10

Technical status. *SOHO* was launched on 1995 December 2 and completed launch and early orbit activities (commissioning) in 1996 March, not long after *SOHO* reached its L1 halo orbit. Just after the end of the prime, two-year mission, control of the spacecraft was lost in 1998 June, and only restored three months later through the heroic efforts of an ESA-NASA-contractor-university team. All twelve scientific instruments were still usable, most with no ill effects. Despite the immediate failure of two of the three onboard gyroscopes and the later demise of the third (in 1998 December), by 1999 February, new, "gyroless" onboard control software not only allowed the spacecraft to return to full scientific usefulness, but actually provided a greater margin of safety for spacecraft operations. *SOHO*'s current margins for thruster propellant (necessary to bleed angular momentum from the spacecraft rate wheels and trim *SOHO*'s halo orbit every few months) and solar panel output are considered by spacecraft engineers to be adequate for considerably longer than the four-year horizon of this proposal.

Instrument status. As noted in Appendix B, all *SOHO* instruments are operational and returning scientific data of high quality. Only a small number of subsystems (*e.g.* the piezoelectric tuning mechanism in the LASCO C1 Fabry-Pérot filter) have degraded or failed to the point that individual sensor heads are unusable. The Appendix gives details on throughput degradation for each instrument.

Science operations. Six of the twelve *SOHO* Principal Investigator (PI) teams are represented by teams resident at the Experimenters' Operations Facility (EOF) and Experimenters' Analysis Facility (EAF) at NASA Goddard Space Flight Center. The TRACE Small Explorer EOF is located in the same building as the corresponding *SOHO* facility, and TRACE is considered the thirteenth *SOHO* instrument for science planning and science operations. A TRACE representative participates in the daily, weekly, and monthly *SOHO* science planning meetings. Day-by-day science planning and operations are labor-intensive, and one of the reasons for the disparity of *SOHO*'s science operations budget in comparison with those of other, existing S3C missions. All of the *SOHO* instruments operated from the EOF are reprogrammed on one- to three-day cycles to match the complexity of tradeoffs made necessary by limited bandwidth from L1. (The LWS Solar Dynamics Observatory mission, set for launch in late 2008, will do away with much of *SOHO*'s short-term planning, as its much higher telemetry bandwidth will not require many such trades.)

The workstations and storage subsystems used in the EOF, both by instrument teams and the EOF Core System (ECS), which distributes realtime and quicklook data at the EOF as well as providing a secure connection for instrument commanding, are beginning to age. While hardware failures are still relatively rare, there are issues in upgrading older hardware to operating system releases that patch security vulnerabilities in accordance with NASA IT security requirements. This issue and the relatively high cost of maintaining aging hardware have led both the Space Science Mission Operations office (Code 444, which is responsible for the ECS) and the *SOHO* Science Working Team, to upgrade, replace, or stockpile replacements for existing EOF hardware and software to insure reliable science operations over the next four to five years.

Both of the primary *SOHO* archive sites (MDI and the SDAC) are members of the group of four sites (along with the National Solar Observatory and Montana State University) on which the Virtual Solar Observatory (VSO) prototype was built. Thus, *SOHO* data are now part of the distributed data environment. In addition, the SDAC is a partner in the European Grid of Solar Observations (EGSO), another effort to provide uniform, network-based access to a wide variety of solar physics data.

Background: management. *SOHO* is a European spacecraft, built for ESA and populated with instruments provided by nine European PI's and three American PI's. (Each instrument has an international complement of Co-Investigators.) *SOHO* is both half of ESA's Solar-Terrestrial Science Programme Horizon 2000 "Cornerstone" (*SOHO* plus Cluster) and part of NASA's Great Observatory. Responsibilities of each agency are delineated in an interagency Memorandum of Understanding, which has recently been renewed. After several Mission Interruption Review Board meetings, ESA and NASA decided to reorganize *SOHO* management by providing the spacecraft with its own program[me] management, instead of matrixing it among other NASA missions operated by Goddard. This arrangement has evolved over the ensuing years, but the Program Manager is still a NASA employee, the director of the Space Science Mission Operations Office, and the Deputy Program Manager is now the lead ESA engineer – for routine science operations; for exceptional operations such as recovery from safehold ("Emergency Sun Reacquisition") and spacecraft maneuvers, their roles are reversed, as ESA bears primary responsibility for the health and safety of the spacecraft. In the seven years this arrangement has been in place, it has dealt efficiently and effectively with a range of minor spacecraft and software problems, as well as the much more serious gyro loss and the malfunction, in 2003, of one axis of the high-gain antenna motor drive. Throughout *SOHO*'s lifetime, ESA management has remained committed to providing the necessary resources to keep *SOHO* operations safe and scientifically productive.

Changes to mission operations, 2006 - 2010. Declining real budgets after FY06, inflation, and the increased cost of operations at Goddard in a "full cost" environment led the *SOHO* project scientist and Program Manager to examine the possibility of decreasing mission operations cost, so that science and science operations would not have to bear the entire burden of the decreased real budget. Based on the experience of the TRACE, ACE, WIND/POLAR, and WMAP flight operations teams with automated mission operations, we will begin engineering a change to "lights-out" (manned only 8 – 12 hours per day, with e-mail and pager notification of anomalies at other times) operations in FY06, with a target start date of the beginning of FY07. We have budgeted (see Table V-1) $300K for this engineering effort in FY06; the effort will come from current members of the *SOHO* Flight Operations Team (FOT). We have budgeted $350K in FY07 as a contingency against possible slips in implementing lights-out operations. Lights-out operations will require the ability to automate downloads (playbacks) from the spacecraft, which will in turn require some changes to onboard software, which ESA is committed to develop. Since the new mode of mission operations represents a departure from the current, high level of staffing, we will require formal approval from ESA and NASA S3C management before implementing the new mission operations mode.

The year of living intercalibratedly. Assuming a launch of SDO in 2008 August, followed by 90 days of commissioning, SDO science operations will start about at the beginning of FY09. During FY09, we will continue to operate MDI and EIT, in order to intercalibrate them against their analogs on SDO (HMI and AIA), while operations of UVCS will be ramped down, and the UVCS team will begin to produce their final data archive. The European PIed instruments, we assume, will continue to operate normally, and LASCO will be operated in a purely synoptic mode, enabling the LASCO PI team to begin final archiving of the first 13 years of observations. Because of simpler coordination considerations, we will reduce our NASA-supplied EOF Core System staff from two Science Operations Coordinators (SOCs) to one.

The SOHO "Bogart" mission, 2010 - 2014. With the completion of MDI and EIT intercalibrations, operation of those instruments will cease, and there will no longer be any need for the *SOHO* EOF. Only LASCO, and any European instrument that can operate without the EOF system and without SOC support, will continue to operate. Management of *SOHO* will pass to the SDO project, as NASA's interest in continuing *SOHO* operations will be based solely on the provision of LASCO coronagraph observations – a critical scientific element of the SDO mission that had to be dropped from the spacecraft for management reasons – and the CELIAS solar wind measurements. *SOHO* will be operated by an FOT similar in size to that for a SMEX mission, or less than a quarter of the current FOT manpower.

Organization of budget proposal Funds for *SOHO* science operations and data analysis, and those for mission operations, are now both nominally the responsibility of the US project scientist. Unlike in previous *SOHO* Senior Review proposals, therefore, we do not break down the two budgets separately.

The nominal, FY06 – FY10 budget is shown in Table V-1.

There are several notable features in the Table. Mission Services decrease in FY07 and FY08 to reflect the smaller FOT necessary for single-shift operations. (As noted above, development lines in FY06 and FY07 will fund the engineering of the new operations method.) Attrition continues to allow savings in the Mission Services through FY09, after which the costs drop sharply as the FOT is scaled back to support no more than six hours of realtime contact per day, which should still allow all service module (spacecraft) commanding as well as two to three LASCO command loads per week to support synoptic operations. Funding for science drops in FY08, but most of the loss is absorbed by the MDI team, whose scientists will by then be transitioning to SDO HMI work. A larger drop in science support occurs in FY09, when UVCS and the LASCO science team also begin to ramp down. (The support level for the US Lead Co-Investigator for CELIAS remains constant in real dollars throughout, since it is already at the minimum level for supporting the scientific data pipeline, and quite modest.) In FY10, the MDI team is funded at a level that should allow completion of their final archive, while UVCS, LASCO, and the US EIT Co-I teams are funded at a level of approximately one post-doc FTE each, to finish archiving, support data users, and complete research already under way. In FY10, the beginning of the "Bogart" mission to support SDO, we assume that no management overhead will be borne by *SOHO*, as the mission transitions to SDO management.

		FY06	FY07	FY08	FY09	FY10
		Budget ($k)	Budget ($k)	Budget ($k)	Budget ($k)	Budget ($k)
1. Development		300.0	350.0			
2.a Space Communications Services		4.4	4.5	4.7	4.8	5.0
2.b Mission Services		4,326.5	3,912.4	3,643.6	3,057.1	1,461.0
2.c Other Mission Operations		300.0	750.0	300.0		
3. Science Center Functions		5,930.7	5,087.1	4,693.1	3,355.3	1,259.5
4. Science Data Analysis		4,760.5	4,245.2	3,914.4	2,933.8	1,189.2
5. E/PO		544.9	511.8	510.2	279.4	128.2
Totals		16,167.0	14,861.0	13,066.0	9,630.4	4,042.9

Table V-1. In-guide budget, FY06 – FY10. The totals for FY09 and FY10 are ***below*** *the guidelines for those years. The development figures in FY06 and FY07 represent the cost of designing and testing the automation of some aspects of mission operations. In FY10, costs are drastically reduced for a "Bogart" mission without MDI, UVCS, or EIT operations but continuing LASCO observations to complement SDO. The totals for FY09 and FY10 are less than the "barebones" guidelines.*

Science data analysis in FY09 and FY10. The budget guidelines for *SOHO* are more than adequate for both of the last two years considered in this proposal. We have therefore budgeted for approximately $984K in FY09 and $5.957M in FY10 to be returned to S3C management, hopefully *for scientific research*, specifically to augment the S3C Guest Investigator program and the extended missions of STEREO and Solar-B. Not only will a number of scientists formerly supported by *SOHO* be seeking funds in those years, but the Phase E MO&DA support for the SDO PI teams was designed to allow little more than pipeline operations after the first 18 months of science operations. If the physics of the solar interior, solar magnetic variability, space weather, and the solar wind are to remain active research areas in the United States, a healthy Guest Investigator program should be the highest priority for funding in *any* year.

"Optimal" budget. As noted above, funding for *SOHO* is adequate at the nominal, "bare-bones" level. We therefore present no higher, "optimal" budget.

VI. Education and Public Outreach

Activities, 2003 – 2005

There have been three principal centers of education and outreach activities during this period: the Stanford Solar Center (SSC, at the MDI home institution), the Smithsonian Astrophysical Observatory (SAO; UVCS), and NASA Goddard. We outline some of the highlights of our activities at each location over the last two and a half years.

Stanford. In conjunction with NSF, the SSC has developed low-cost (~$150) space weather instruments that monitor and track changes to the Earth's ionosphere caused by solar activity. The monitors were designed and developed by teacher interns over a two-year period and beta-tested in local, minority-serving high schools. 100 monitors, funded by MDI's NASA grant, are currently in production, to be distributed to high school and community colleges throughout the nation. The hope is to provide experience with hands-on science and generate enthusiasm for science and technology amongst young people, with a key target being students from under-represented groups. The International Heliophysical Year (IHY), 2007, Organizing Committee and the United Nations have designated our Space Weather Monitors as supported projects of the IHY. The hope is to place five of these low-cost monitors in each of the 191 nations of the (UN-designated) world. Funding is being sought from private foundations.

Poster-spectroscopes, previously developed with MDI funding, continue to be extremely popular. During the last two years, the instrument has been redesigned and reprinted so it can be distributed flat format (instead of as a rolled up poster), 11"x17" size, and perforated for punch-out. Class-size packets of spectroscopes are provided to teachers through the nation. To date, we have distributed roughly 40,000 spectroscopes. John Beck, an MDI team scientist, has helped develop and present workshops for teachers throughout the state. Spectroscopy is a key topic for these workshops, and John has taught middle and high school science teachers how to make and use our foldable spectroscopes.

MDI team members continue to give a variety of workshops to local elementary, middle, and high school students. New additions in the last 2 years include Science Nights for elementary schools, Take Your Sons and Daughters to Work spectroscope workshops, SUCCESS Summer Camp workshops for under-served middle school girls, Reach for Tomorrow workshops for underserved students nationwide, short activity workshops for Community Day at Stanford, as well as the occasional teacher-requested spectroscope workshop for local schools. During the last year we expanded our repertoire by adding planetarium programs using a portable StarLab planetarium. In conjunction with the Lawrence Hall of Science, we are currently developing a solar-science based program designed for use in small, interactive planetaria.

MDI scientists have also provided information on communicating information about the Sun to Park Rangers at a SECEF-organized workshop for the National Park service; developed a Website section on Native American medicine wheels for the 2005 Sun-Earth Day program.

SAO. The UVCS team has partnered with Southern University at Baton Rouge (SUBR), home of the largest HBCU undergraduate physics program, to create a lectureship and summer research internship program. The ongoing collaboration has reached more than 100 SUBR students who have attended the space science lectures provided by UVCS scientists. Two Southern students have participated in summer research projects at SAO. The students start with tutorials on solar science and UVCS data analysis before they get involved with analyzing UVCS data. In addition, students learn how to give talks and write scientific papers.

In the past two years, UVCS scientists participated in three education workshops: Solar and Space Weather materials were presented at a workshop for K-9 teachers held at SAO; in partnership with the COSI (Columbus, Ohio) organization, the UVCS team provided *SOHO* materials along with a video conference presentation on space weather that was delivered simultaneously to classrooms at

four different high schools; and a UVCS scientist was asked to present via the Internet, *SOHO* science topics to educators in Korea.

UVCS scientists provided interviews and materials for use in a middle school earth science textbook (Prentice-Hall), and the UVCS PI also wrote a Space Weather article that was published in an encyclopedia of science and technology (McGraw-Hill). UVCS scientists also provided talks on space weather at the Boston Museum of Science and the Smithsonian Institution in Washington.

NASA Goddard. We have conducted two model collaborations targeting educators and students: FiMS (Fellowships in Mathematics and Science), a partnership grant with the Pennsylvania Department of Education in three school systems, in which *SOHO* educators and scientists work with teachers to increase content knowledge and support their ability to develop and implement inquiry-based lessons that are tied to state standards and the current curriculum; and the Endeavour program, a collaboration between *SOHO* and 18 school systems in Pennsylvania, gives teams of students real-life NASA problems to research. One of the problems involved *SOHO*. Students are supported by teacher team leaders who have been exposed to the content and training through professional development. This has involved several video conferences, several presentations by *SOHO* staff, and a number of meetings. One or both of our E&PO staff attended the New York Science Teachers Conference in southern New York, the NSTA Conference. The *SOHO* media specialist presented a workshop on hands-on outreach at the Astronomical Society of the Pacific meeting (2005 September).

The most significant educational product developed in these years is *Touch the Sun*, a NASA Braille book with *SOHO* and TRACE images, written by Noreen Grice and published by the National Academies Joseph Henry Press in 2005 September. The *SOHO* media specialist provided the visible images (all but one from *SOHO*), which are printed over embossed, tactile images produced by a new technology whose development was funded by *SOHO*. Most of the initial press run will be distributed, free, to blind middle schools students by the National Federation for the Blind. The *SOHO* media specialist and US project scientist helped to edit the text, which was refereed by members of the National Academy of Sciences.

Approximately 0.4 FTE of a professional educator on the *SOHO* staff was dedicated in FY04 and FY05 to producing, with the collaboration of WARD's Scientific, a "kit" of space weather materials for use in classrooms, and emphasizing the role of the magnetic field. Although the educator is no longer on staff, and WARD's has delayed the introduction of the kit, we plan to continue our work with them to make the product available.

The *SOHO* CD-ROM, *Exploring the Sun*, was expanded and updated in 2003 with new video, images and information; 15,000 more were produced. A new edition of *The Dynamic Sun* CD-ROM, with multimedia presentations at multiple grade levels on both English and Spanish, ahs also been produced; total production is now 150,000. Both CD's are distributed primarily at teachers' conferences. The *Sun as Art* exhibit, containing art based on *SOHO* and TRACE images, has been shown at several locations around the US. Each framed image has a caption to explain the science involved in what the viewer is seeing.

Outreach. The *SOHO* Website continues draw considerable interest (> 13,000,000 hits per month), and the near-realtime images and video on the site are displayed in museums and other Websites worldwide. New features in the last six months include Spotlight (focusing on an individual or group doing astronomy), SunWorks (a monthly art contest with solar themes for children and young adults), and the *SOHO* Comet Contest to predict the perihelion of the 1000th comet discovered by *SOHO*, which drew nearly 10,000 contestants worldwide. *SOHO* video and images remain in demand for NASA press releases and "portal" communications, as well as distribution to museums nationwide.

We have produced three different lenticular featuring animations of real solar and auroral data to communicate the Sun-Solar System connection in a dramatic fashion; over 300,000 of these have been distributed.

Proposed work, FY05 – FY10. We propose to continue our education and outreach efforts, as described above, at Stanford and SAO, including a new Out-of-School Time (OST) program, designed to increase the number of underrepresented K-12 students in Boston students choosing careers in science, technology, and mathematics (STEM). Similarly, we propose to continue our outreach efforts at Goddard, although scaling back from 1.0 FTE to 0.5 FTE of media specialist time to reflect the leading role that STEREO will assume in S3C image and video production. Our education effort will focus on science driven education where individual missions contribute to science understanding but do not take center stage in any one program.

To increase the impact of our decreased funding, we will partner with S3C missions at Goddard – *SOHO*, RHESSI, Polar, Geotail, and Wind – and the Sun-Earth Connection Education Forum (SECEF). The STEREO and SDO project scientists have agreed to join this effort as well, as their missions enter Phase E (MO&DA). We propose to develop cross-mission themes and EPO programs and products developed by the individual mission and instrument team EPO programs. By joining the efforts of several missions, we hope to eliminate duplication of effort, leverage award winning resources already in operation, and increase the impact of limited EPO funds for any individual mission. In addition, our approach ensures a sustainable, science-driven EPO program that is more usable in schools and more understandable by the general public.

Existing SECEF Program	How it will be used	Annual Impact
Sun Earth Day 2006 and beyond	Use mission data to help in under-standing the Sun and eclipses…	10's of Millions
Student Observation Network	Develop problem-based learning modules based on mission science	>10,000 students
Space Weather Center	Design and build a museum kiosk on the Sun	>10,000 museum goers, >100 teachers per year in exhibit-based workshops

Table E-1. Existing SECEF programs we propose to use in cooperation with other, Goddard-based S3C missions.

We will employ SECEF's well developed network of end users consisting of museums and science centers; national parks; Girl Scouts USA; amateur astronomers (*e.g.* Astronomical League, AAVSO), and numerous minority and professional groups such as AGU, AAS, La Raza, World Hope, National Society of Black Engineers for informal education. We will use these established relationships to enhance the reach and impact of these programs.

SECEF has extensive experience developing award winning EPO programs that meet both science and pedagogy standards and are reviewed by NASA. Examples of these programs are Sun-Earth Day, the Student Observation Network, and the Space Weather Center. SECEF will incorporate SEC mission science results into programs like these that reach tens of millions of students, teachers, civic groups (*e.g.* Girl Scouts) and general public each year. The table outlines our largest programs and how we plan to incorporate SEC mission science.

Working through the Student Observation Network and SECEF's existing partnership with the Challenger Centers, we will develop grade appropriate, standards-based Problem Based Learning (PBL) modules that will require hands-on analysis of mission datasets in order to solve the problem presented, and we will provide training on the integration of the PBLs into curriculum. We will also work with other mission directorates to develop Exploration-related PBLs involving topics such as planetary magnetospheres, radiation effects on human presence in space, and interstellar winds and magnetic fields.

Evaluation. As members of the NASA Space Science Education Support Network, SECEF's products and programs are reviewed annually for science content accuracy and currency and for pedagogy. We will leverage these existing NASA evaluation programs to ensure S3C education products and programs are engaging, effective, and appropriate for the target audiences.

Sustainability. To ensure sustainability of our programs, we will have the support of the upcoming STEREO (to be launched in 2006) and SDO (2008) missions. As existing missions are terminated, we hope thus to insure steady funding for a healthy, S3C education effort at Goddard.

Category	FY06	FY07	FY08	FY09	FY10
1. Direct Labor (salaries, wages, and fringe benefits)	379.2	355.6	354.4	193.6	89.1
2. Other Direct Costs:					
a. Subcontracts					
b. Consultants					
c. Equipment					
d. Supplies					
e. Travel	10.0	10.0	10.0	6.0	2.5
f. Other					
3. Facilities and Administrative Costs	165.7	146.2	145.8	79.8	36.6
4. Other Applicable Costs					
5. Subtotal--Estimated Costs	554.9	511.8	510.2	279.4	128.2
6. Less Proposed Cost Sharing (if any)					
7. **Total E/PO Estimated Costs**	554.9	511.8	510.2	279.4	128.2

Table E-2. The SOHO education and outreach budget for FY06 – FY10. The FY05 budget was approximately 0.5 FTE higher: the SOHO media specialist will henceforward be working halftime on STEREO. The budget includes personnel at Stanford University, the Smithsonian Astrophysical Observatory, and NASA Goddard, in a roughly 1:1:3 ratio. From FY06 to FY08, we expect to be able to contribute nearly 0.5 FTE worth of funding to a consortium effort involving SECEF and several other S3C missions at Goddard (see text). After FY08, we expect to have to begin to reduce our E&PO effort.

FiMS and Endeavour. To the extent that our resources allow, we will continue our alliance with Pennsylvania schools to deliver inquiry- and problem-based education programs based on S3C mission science.

Appendix A. *SOHO* publication record, 1996 – 2005Q3

SOHO refereed publication rates through the third quarter of calendar year 2005, can be found in Table A-1.

Calendar Year	**Ref. Journals Only**
1996	31
1997	126
1998	174
1999	297
2000	294
2001	209
2002	287
2003	301
2004	326
2005Q1-Q3	238
Total	2,283

Table A-1. SOHO refereed papers

Here, a "*SOHO* paper" is taken to mean any paper using *SOHO* data, or concerning models of theoretical interpretations of *SOHO* measurements.

"Market share" In the years since the launch of *SOHO*, there have been over 2,300 different authors and co-authors of *SOHO* papers in refereed journals. Since *SOHO* carries both *in situ* and remote sensing instruments, there is a large potential pool of authors. Considering just the remote sensing instruments, there are roughly 600 members of the AAS Solar Physics Division and a roughly equal number of active solar physicists in Europe and Asia (combined). Past experience indicates that approximately 75% of those are "active," in the sense of publishing at least one refereed paper per year, so *SOHO* is clearly serving a large number of members of the heliospheric community as well.

Publication rate. Despite reduced funding for scientific analysis of *SOHO* data both in the US and the countries of the European Principal Investigators, the *SOHO* publication rate has actually risen slightly over the last three years.

We are convinced that this success is based on the open and convenient accessibility of *SOHO* data and analysis software. Only a data policy of this type is likely to draw in the widest possible scientific community — including amateurs — to the enterprise of mining S3C data for their maximum scientific return.

Bibliography. A listing of *SOHO* publications in refereed journals for the years 2003 – 2005 can be found at http://umbra.nascom.nasa.gov/soho/sr05/soho_publ_2003_2005.html .

Appendix B. Instrument Status as of 2005 September 20

GOLF

- Operating nominally, with data continuity ~98% outside *SOHO* 1998-1999 "vacation" periods, including no losses during telemetry "keyholes"
- Overall throughput down by a factor of <5 since launch, but:
  - largest noise source is the Sun itself, so negligible adverse effect over most of the frequency range, including that in which the *g*-modes are expected
  - significant reduction in signal to total noise ratio in a region around 1 mHz
- No reason to doubt that GOLF can continue to function in its present mode for several years
  - Complete redundant channel still available, though unused since initial, on-orbit commissioning

VIRGO

- All VIRGO instruments (the two types of radiometers: PMO6V and DIARAD, the filter radiometers SPM, and the luminosity oscillation imager LOI), are fully operational and performing properly. The degradation of sensitivity is still relatively small and all the instruments are still able to achieve the same accuracy and precision as at launch.

MDI

- ~90,000,000 images; after on-board computations, ~15,000,000 raw data images downlinked
- Expected degradation in total light throughput due to changes in the front window; compensated *via* increased exposure time. Through 2005 June:
  - total degradation: 33%
  - mean annual degradation: 4%
- Exposure time uniformity: sudden drop in 2000 March, from a part in 12000 to a part in 4000
  - affects helioseismology only for $l < 4$
  - adds some noise to zero point of photospheric magnetic field measurements; correctable
  - No variations above the one part in 4000 level since 2002 February reduction in optics package temperature
  - No detected change in the CCD flat field except for variations with focus change
- The drift in central wavelength of the Michelson's has nearly stopped
- The drift in best focus position has moved the nominal focus setting back almost to the design point. Shortly after launch it was at the limit of the adjustment range.
  - This drift has also apparently slowed
- In summary, no known limit to MDI's useful life

SUMER

- Pointing mechanism has worked flawlessly during the recent years and restrictions on pointing will be released, since detector lifetime is regarded as the most critical resource
- Detector A can only be operated with reduced spatial resolution (MCP exhaustion)
- Detector B fully operational and will remain radiometrically calibrated for another 2-3 years, based on extrapolation from past performance

CDS

- GIS nominal; no recalibration or changes to high voltages have been necessary in the past 3 years.
- NIS nominal; microchannel plate current anomaly in 2005 July appears to have been self-healed after a series of tests and is being used for regular observations again
- Electronics nominal; trending shows no aging of components
- Mechanisms: Some 'stickyness' when rastering the GIS slits necessitated a small restriction on the range of movements. This has now been compensated for by improved ground planning software that moves the allowed range of movements to outside of the restricted area. This issue no longer impacts on science. All other mechanisms continue to operate nominally.
- Thermal: As with all other components of *SOHO*, the sunward side of CDS shows a secular increase in temperature, but analysis of the science data shows that the NIS wavelength calibration remains within tolerances.
- Onboard software: No issues

EIT

- EIT is nominal
- Instrument throughput decrease stopped and reversed since 2003 (see: http://umbra.nascom.nasa.gov/eit/eit_guide/euv_degradation.html)
  - Reversal due to long bakeouts occasioned by telemetry keyholes
  - CCE loss can be tracked accurately with calibration lamp images
  - Degradation now understood and modeled
  - Present exposure times range from 12 s (195 Å) to 2 m (284 Å): lots of latitude left
  - Current throughput at 195 Å is comparable to that in 2000 January

UVCS

- O VI detector: Detector efficiency loss only in a localized region near the center of the detector; has had only a minor impact on science. Further aging has been brought to nearly a standstill by a reduction in the detector temperature.
- Ly a detector: High voltage (HV) off most of the time since 1998 November because the HV current was unacceptably high. With the development of an operational technique to reduce detector temperatures, it was recommissioned in summer 2005. The detector is fully operational, and is being used for suprathermal seed particle population measurements.
- Visible light detector: Experienced an anomaly in its housekeeping telemetry system and was turned off in 2004 April. Since its principal function of verifying the LASCO electron density measurements and co-registration has been accomplished, the risk of further operation is not justified.
- Mechanisms: All mechanisms continue to behave nominally except for the Ly a grating drive, which is slow to respond when commanded; has not prevented this channel from being used for high priority science.
- Response: Changes in system radiometric response are being accurately tracked using observations of stars. The changes depend on the unvignetted aperture used for observations at various heliographic heights. For example, the current in flight calibration is within 60% of the laboratory calibration for observations at 2.5 R_{Sun}.

LASCO

- Thernisien *et al.* (2005) have performed a detailed analysis of the intensity of a set of about 50 moderately bright stars that transited through the C3 field of view

- These 50 stars generated about 5000 observations during the lower cadence in the first three years of *SOHO* operations and about 15000 observations thereafter
- All stars have spectra well known from 13-color photometry
- Using these stellar spectra as standards and the observed LASCO count rates, derived the photometric calibration factors of the C3 coronagraph for all five color filters with an absolute precision of ~7%
- Decrease in the instrument sensitivity found to be only ~3.5% over the 8 years studied or < 0.5% per year

- C2 response changes similar; still under investigation
  - Final calibration expected before end of 2005
- The Fabry Pérot interferometer in the C1 coronagraph did not survive the extreme cold the instrument experienced (-80C) during the 1998 *SOHO* offpointing

CELIAS

- MTOF/PM, STOF/HSTOF, SEM nominal
  - MTOF, PM efficiency degradation of 2 (Fe) to 5 (H); still extremely high S/N
  - STOF performance stable, MC degradation compensated for by increase in HV
- CTOF impaired since 1996 October (HV power supply hardware failure)

COSTEP

- COSTEP consists of two sensors, the Low-Energy Ion and Electron Instrument (LION), and the Electron, Proton, and Helium Instrument (EPHIN). Both instruments have been working very stably during the last three years without major degradation. Detector degradation during the first year of the mission could be largely recovered by additional programming and calibration effort. The COSTEP experiment still fulfils its scientific goals with minor degradation in resolution for a few energy channels.
  - **LION:** Despite the unexpectedly high noise level in the LION detectors since shortly after launch, detailed analysis shows that the scientific goal for LION can be achieved by using additional calibration and calculation, though with the disadvantage of a higher trigger level for small events. Otherwise, LION remains nominal.
  - **EPHIN:** Detector E of the EPHIN instrument showed steadily increasing noise levels throughout 1996, and had to be switched off (on 1996 October 31) to guarantee reliable measurements with the instrument in the future. By changing the instrument configuration, the measurements of EPHIN can still be achieved with slightly degraded resolution. No significant degradation of the scientific goals of EPHIN are caused by this detector failure

ERNE

- Secular increase in temperatures at front of spacecraft has caused increased detector leakage currents. Including radiation effects, the increase during the last five years has been roughly 20 $\%yr^{-1}$.

- One of the detector channels of the topmost ERNE/HED detector layer malfunctioned on 2000 November 21. Updated onboard software accounts for this issue: the geometrical acceptance (view cone) of the detector is unaffected, as is the measurement of the heavy nuclei (Carbon and heavier). Also the light nuclei are unaffected up to an energy of ~ 20 MeV/n. Between 20 MeV/n and 120 MeV/n (maximum energy measured by ERNE), both the coordinate and energy values of the affected detector become increasingly unreliable. This, however, ahs no effect on particle identification and produces only marginal statistical

fluctuation on the total energy of these particles that deposit most of their energies in the lower detector layers.

SWAN

- Instrument status unchanged since 2001
  - All four motors nominal
  - +Z hydrogen absorption cell nominal; -Z cell empty: no absorption when activated (loss occurred in 2001)
  - Both sensors calibrated using HST STIS reference spectra: +Z sensor response constant since 1998 (outside of adjustments for high voltage [HV] setting), -Z sensor response shows decline of ~ 10% per year. HV setting changed to compensate as much as possible

Appendix C. Acronyms

CDS	Coronal Diagnostic Spectrometer
CELIAS	Charge, Element, and Isotope Analysis System
CISM	Center for Integrated Space Weather Modeling (NSF supported)
COSTEP	Comprehensive Suprathermal and Energetic Particle Analyzer
CTOF	Charge Time-Of-Flight sensor of CELIAS
DIARAD	DIfferential Absolute RADiometer (active cavity radiometer) component of VIRGO
EAF	Experimenters' Analysis Facility
EIT	Extreme ultraviolet Imaging Telescope
ERNE	Energetic and Relativistic Nuclei and Electron experiment
EOF	Experimenters' Operations Facility
ESA	European Space Agency
EUV	Extreme ultraviolet
GIS	Grazing Incidence Spectrograph of CDS
GOLF	Global Oscillations at Low Frequencies
HBCU	Historically Black College and University
HIDE	Heavy Ion Depletion Event
IP	Interplanetary
LASCO	Large-Angle and Spectrometric Coronagraph
LOI	Luminosity Oscillations Imager component of VIRGO
MDI	Michelson Doppler Imager
MTOF	Mass Time-of-Flight mass spectrometer of CELIAS
NIS	Normal Incidence Spectrograph of CDS
PM	Proton Monitor of CELIAS MTOF
PM06	Twin-cavity radiometer component of VIRGO
RHESSI	Ramaty High Energy Solar Spectroscopic Imager
S3C	Sun-Solar System Connections
SDO	Solar Dynamics Observatory
SEM	Solar EUV monitor of CELIAS
SEP	Solar Energetic Particle
SMEI	Solar Mass Ejection Imager
SOHO	Solar and Heliospheric Observatory
SOI	Solar Oscillations Investigation
SMEX	Small Explorer
SPM	Spectral irradiance monitor component of VIRGO
STEREO	Solar TErrestrial RElations Observatory
STOF	Suprathermal Time-of-Flight ion telescope, part of CELIAS
SUMER	Solar Ultraviolet Measurements of Emitted Radiation (UV spectrometer)
TRACE	TRansition Region And Coronal Explorer
SWAN	Solar Wind Anisotropies
UVCS	Ultraviolet Coronagraph Spectrometer
VIRGO	Variability of Solar Irradiance and Gravity Oscillations
VSO	Virtual Solar Observatory

SOHO instrument names are in blue.